Emergent Materials (2022) 5:489–508
https://doi.org/10.1007/s42247-022-00356-0

REVIEW

Review on role of nanoscale HfO_2 switching material in resistive random access memory device

Napolean A[1] · **Sivamangai NM**[1] · **Rajesh S**[1] · **NaveenKumar R**[1] · **Nithya N**[2] · **Kamalnath S**[3] · **Aswathy N**[4]

Received: 11 November 2021 / Accepted: 26 January 2022 / Published online: 28 February 2022

Abstract

Typical semiconductor data storage devices reach a breaking point in terms of their physical dimension and storage capacity. Among various upcoming high-density non-volatile memories, resistive random access memory (RRAM) shows a potential candidate for upcoming ultra-high-density memory applications, due to its speedy, low power consumption and a matured metal–insulator-metal (M-I-M) structure. In this structure, metal oxides serve as the insulator has demonstrated the potential to serve as viable resistive switching memory applications. Across a range of material systems, transition metal oxides (TMO), HfO_2-based RRAM cell type has demonstrated better complementary metal oxide semiconductor (CMOS) compatibility and outstanding device performances. This article signifies the narration of HfO_2 materials RRAM cell and pointing to upgrade the resistance switching uniformity and device variability performance. The review focuses on various resistive switching principles, geometry, device structuring, materials selection, and forming process which plays the critical characters in determining the device performance have been reviewed. We also provide possible solutions to increase the switching stability, endurance, and retention and reduce the forming voltage through the optimized device modifications. The review ends with summarizing different HfO_2-based RRAM devices' experimental performance and the future research scope.

Keywords HfO_2-based RRAM · Conducting filament · Oxygen vacancy · Switching uniformity · Reliability

1 Introduction

NAND flash memory is reaching its miniaturization extent [1] the semiconductor industry has developed progressively involved in other substitute technologies which have developed scalability, very fast, larger endurance, and lesser operating power compared to conventional memory. In the latest periods, rising new technologies like phase change random access memory (PCRAM) [2], magnetic random access memory (MRAM) [3, 4], ferroelectric random access memory (FeRAM) [5], and RRAM [6–16] have been suggested to afford greater memory device density. Among these, RRAM is the most capable one owing to its quality of cost-effectiveness, quick switching speed, and great compatibility with the CMOS procedure [10–12].

In RRAM, the basic device construction is denoted as the MIM structure; the switching principle is changing the insulator material layer (resistance switching layer) resistance value by applying voltages between two electrodes. A low resistive state (LRS)/set and high resistive state (HRS)/reset in the dielectric material can be reached periodically by proper supply voltages to the electrodes. In general, for

---

✉ Napolean A
nepojustin@gmail.com

Sivamangai NM
nmsivam@gmail.com

Rajesh S
drsrajesh@karunya.edu

NaveenKumar R
naveentamil256@gmail.com

Nithya N
nithyaame@gmail.com

Kamalnath S
kamalnath2021ias@gmail.com

Aswathy N
aswathy.ec@adishankara.ac.in

[1] Karunya Institute of Technology and Sciences, Coimbatore, India

[2] Kumaraguru College of Technology, Coimbatore, India

[3] Nandha Engineering College, Erode, India

[4] Adishankara Institute of Engineering and Technology, Kalady, India

resistance switching (RS) layer, perovskites [17], chalcogenides [18], binary metal oxides [19–23], and nitrides [24] are obtainable. Across various RS layers, due to the easy manufacturing procedure, the binary transition metal oxides are expansively learned for the RRAM devices [19–23].

Through the binary transition metal oxides, HfO_2 materials are desired due to their highly productive and decent characteristic with the CMOS technology. Specifically, HfO_2-based conductive filament (CF) RRAM is the best demonstrative type. It has extraordinary memory performance [25–27]. The source of the RS in HfO_2 is depending on the establishment and distraction of a CF produced by the migration of the oxygen vacancies (Vo) within the switching layer [28]. Recently HfO_2-based RRAM has been intensively explored as a feasible possible choice for upcoming non-volatile memory [29] or neuromorphic computing devices [30].

This article concentrates on HfO_2-based RRAM and examined its predictable RS principles, materials selection, dissimilar device structures, and important parameters which impact device performance. Moreover, we summarized the experimental data which denoted the technical past development in an HfO_2 RRAM. Also, we analyzed the techniques to enhance the device uniformity and reliability, by dipping forming voltage, and various device structures with suitable fabrication techniques. This article ends with an evaluation of the future research development for the HfO_2 RRAM devices.

2 Basic principles of resistive switching

The basic RS principle in HfO_2 RRAM is based on the device resistance level changing between two finite resistance values (HRS and LRS) when required electric stress applied between two metal electrodes. The resistance value changed from HRS to LRS is called the set condition. Similarly, resistance changed from LRS to HRS is denoted as a reset condition. Even after the applied voltage is detached, the cell maintains its previous resistance value, which is the core principle of the non-volatile RRAM switching principle. All individual HfO_2 memory cells required a one-time electroforming/forming voltage [31] need to initiate the switching process. The basic forming, set and reset operations are shown in Fig. 1.

Mostly, all HfO_2-based RRAM cells are broadly working in two operating modes, unipolar and bipolar modes as indicated in Fig. 2. These modes are dependent on the applied voltage polarity for a set and reset process; in a unipolar mode, the set and reset conditions occur in the same voltage polarity directions at different voltage amplitudes. Bipolar mode operation is depending on the applied voltage polarity in which set and reset operations are achieved in opposite polarity voltage values. In both modes, to prevent the device from a permanent dielectric breakdown, optimized compliance current (CC) value is applied. Also, to retrieve data (read operation), a minimum voltage is required without any effect on the cells' HRS and LRS level change [31].

We introduce the general classification in an RRAM. Broadly, three types of RS principles are involved in RRAM switching operation. (1) Creating a CF build by Vo migrations in the SL. Most of the binary metal oxides (including HfO_2) are under this category called oxide-based RRAM. (2) The CF is composed of metal atoms, represented as conductive bridge resistive random access memory (CBRRAM). (3) Electronic mechanism in which charge trapping/de-trapping function is responsible for the resistive switching.

2.1 Oxide-based RRAM

In an oxide-based RRAM, the oxide defects are common in nature due to the defects Vo produces. The Vo concentration and distribution can affect the electrical resistance of the materials. In most of the semiconductor oxides, Vo acts as donors. Developing and relocation of anions/cations cause

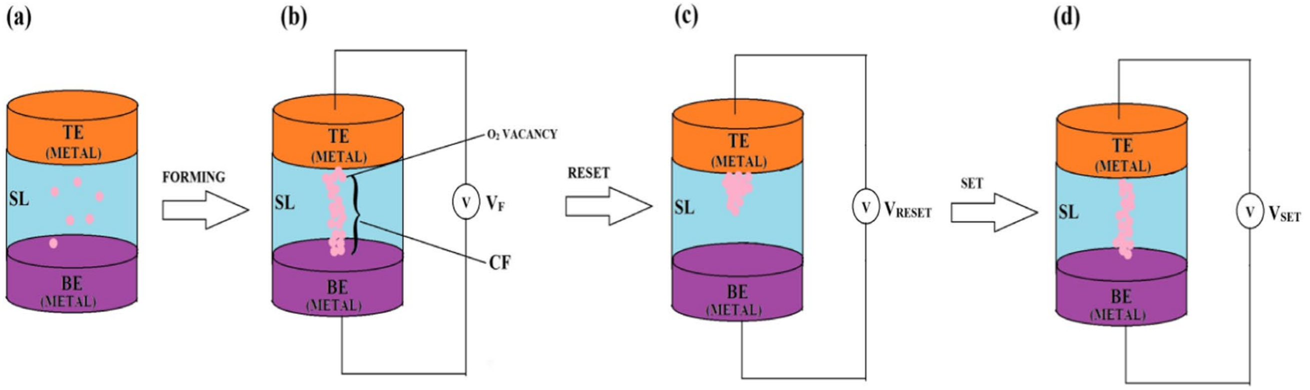

Fig. 1 Basic RRAM structure with forming, set and reset operation

Fig. 2 RRAM switching modes

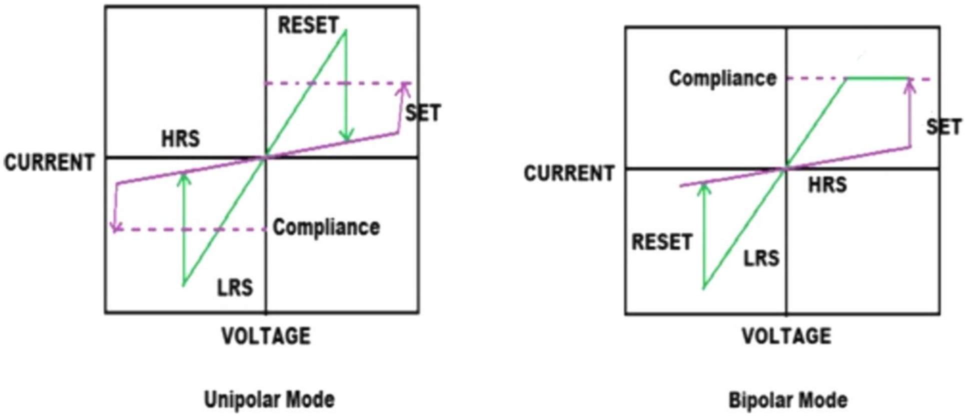

Unipolar Mode

Bipolar Mode

a valence change of the ions. This point defects migration is known as valence change memory. Generally, charge defects movement produces a switching (bipolar) mechanism, when the external field is high. For better resistance switching (resistance value changes from high to low or low to high), considerable point defects are needed. A combination of defects started the cluster formation, producing a conducting filament. HfO_2 RRAM is mostly working based on this Vo movement of CF logic. In the M-I-M structure, when the positive electric field is applied on the top electrode, conducting filament rupture/formation is produced by the action of Vo movement in up and down direction as shown in Fig. 3. The set and reset are strongly dependent on the formation and rupture of Vo. Beyond this basic operation, Vo plays a varied role in RS, which can be explained by the following three ways,

(1) The CF is created due to the cluster of Vo when the electric field is applied in between electrodes. (2) In some M-I-M structures, the applied voltages in between metal electrodes build an interface layer (IL). Also, based on the work function difference of electrode and oxide layer, the Schottky barrier is produced. This barrier height can be modulated based on the Vo concentration and distribution. The height deviation switches the electrical resistance of the device. (3) The Vo can create and trap vacancy for the electron in the Schottky barrier region. Once the electrons are trapped in the trap vacancy which is created by Vo, due to neutralization, the Schottky height is modulated, which yields the RS effect.

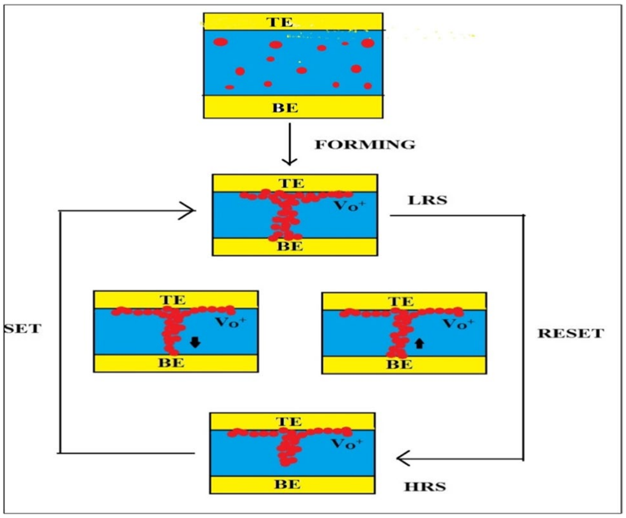

Fig. 3 RS mechanism in oxide-based RRAM

Based on the mobile ions type and its migration, the RRAM switching mechanism are classified into three major categories: (i) cation RRAM (when we use active electrode metal, CF formation only by the cations-commonly known as electrochemical metallization memories (ECM); (ii) anion RRAM (CF formation only by anions like oxygen vacancy-most common in transition metal oxides-known as valence change memories (VCM); (iii) dual ionic RRAM (CF creation depends on both cations and anions).

Wedig et al. demonstrated in transition metal oxide semiconductors, and the CF creation does not only depend on the Vo. In addition to that, it is based on host cation movement of Ti, Hf, and Ta in TiO_2, HfO_2, and Ta_2O_5 respectively. These combined anions (Vo) and host cations lead to resistive switching in oxide-based M-I-M structures. Results concluded that, by appropriate usage of the interface layer, RRAM switching is converted from VCM to ECM switching operation [32]. Figure 4 represents the set function by both anion and cations in HfO_2 film. These two mobile ion barrier energy values play a role in initiating the switching process.

[33]. Recently, Wen Sun et al.'s review article showed a detailed analysis regarding dual (CF formation by both Vo and host oxide cations) ionic devices [34]. Moreover, H'ector García et al. present set and reset switching transitions are controlled over by the capacitor instead of a conventional voltage or current controlled switching operation. In this way, the CF filament is easily controlled by two independent parameters (voltage and discharge time) of a discharging capacitor [35]. Napolean et al. reviewed the significance of compliance current (CC) value plays in

Fig. 4 CF formation by Vo and cations [32]

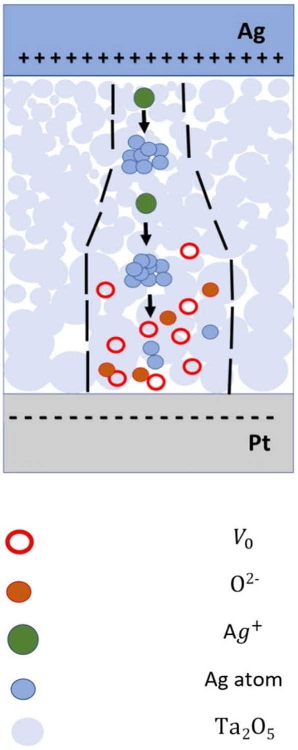

CF width, switching voltages, and reliability of the memory cell [36].

2.1.1 CBRAM

In some MIM structure, when one oxide reactive metal electrode (Cu^+) is kept in an intermediate electrochemical potential value, movable cations undergo the electrochemical redox reaction and lead to bipolar switching. The set progression is a result of metallic filament creation and the resetting phenomenon stands on the termination of the metallic filament as explained in Fig. 5 [37]. The entire set and resetting process are explained as, initially, when a positive voltage is applied on TE, oxidation occurs; it creates Cu^+ and electrons shown in Fig. 5b. Cu^+ ion movements initiate the reduction process. After reduction, Cu metal atoms are accumulated from BE to TE. It builds a CF in between electrodes, yields a set condition depicted in Fig. 5c. After a negative voltage is applied on TE, again oxidation happens, it breaks the CF, and the device becomes reset condition mentioned in Fig. 5d.

2.2 Electronic switching mechanism

In this method, CF is created due to ion movements and the redox concept. Charge trapping/de-trapping–dependent devices are operating based on an electronic mechanism. Odagawa et al. showed the Pt/PCMO/Ag RRAM cell RS is explained by trapping and de-trapping of charge carriers/holes since the PCMO-centered cells obey the trap controlled space charge limited current (SCLC) principle. These trap-filling and trap-de-filling methods owing to the powerful electron relationship perform a vital effect in the RS phenomenon.

2.3 Oxygen vacancy theory and modeling

Various switching theories/simulations are used to describe the Vo generation, recombination, and diffusion processes in the above-mentioned three switching mechanisms. In RRAM, the microscopic physics depends on point defects and further creation/rupture of CF in a

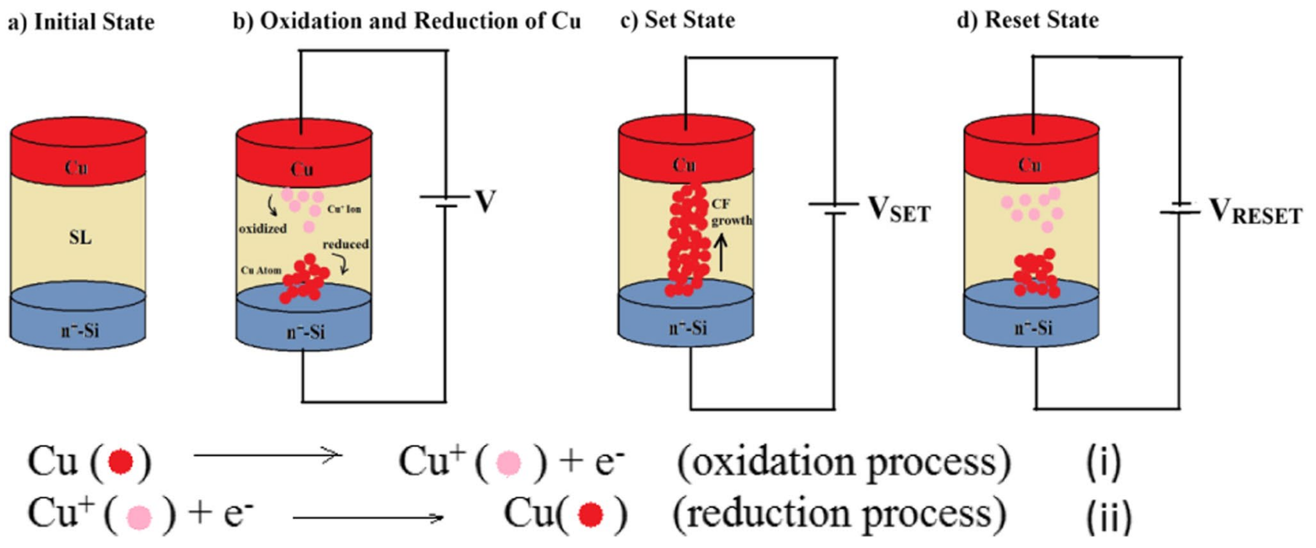

Fig. 5 (a–d) Basic switching action of CBRAM

switching layer. Vo and CF formation theory help the researcher to move towards successful switching modeling. Yuehua Dai et al. demonstrated the effects of microscopic parameters like crystal orientation and doping concentration on the CF formation in HfO_2-based RRAM. They concluded out of ten crystal orientations only in four orientations (011, 100, 010, and 001) CF is produced. Also, they analyzed the RRAM metrics for different stoichiometry values. $HfO_x = 1.875$ (Vo concentration is 4.16%) gives reduced operating voltages and high uniformity. Below 4.167% of Vo concentration, RS is absent. Recently, Desmond et al. described the switching model by relating the microscopic parameter of activation energy, Vo density (nd) with a macroscopic parameter of switching voltages, and hopping current conduction mechanism. Results are validated with a kinetic Monte Carlo (KMC) simulation. In the set function, the rate of Vo and oxygen ion creation is given by [38]

$$G_F(x,y,z) = \vartheta.\exp\left(-\frac{E_A - p_0\cdot\left[\frac{(2+k)}{3}\right].F(x,y,z)}{k_B.T(x,y,z)}\right) \tag{1}$$

ϑ- effective vibration frequency, E_A—energy required to break the Hf–O bond.

F—applied electric field, p_0—dipole moment of HfO2, k—dielectric constant relative to air.

In reset operation, the diffusion rate and recombination rate equations are given in Eqs. (2) and (3)

$$R_D(x,y,z) = \vartheta.\exp\left(-\frac{E_{A,D} - K_D.F_{EFF}(x,y,z)}{k_B.T(x,y,z)}\right) \tag{2}$$

$$R_R(x,y,z) = \vartheta.\exp\left(-\frac{E_{A,R}}{k_B.T(x,y,z)}\right) \tag{3}$$

R_D—rate of diffusion, $E_{A,D}$—Activation energy in a diffusion process, K_D—material property related to HfO_2, F_{EFF}—diffusion direction electric field, R_R—rate of recombination, $E_{A,R}$—activation energy during recombination process. Moreover, the developed Vo diffusion process is controlled by inserting a metal layer between electrodes and metal oxides. Linggang Zhu et al. demonstrated point defects are modulated by the addition of graphene in between TE and SL. Graphene blocks the atom diffusion, which leads to the change in the formation energy of Vo at the interface is measured [39],

$$E_f = E_{\text{interface}}(n\text{Vo}) - E_{\text{interface}} + \frac{n}{2}E\left(O_2\right) \tag{4}$$

$E\left(O_2\right)$—oxygen molecule energy, nVo—total number of Vo.

In an ECM mechanism type, atom diffusion from active metal electrode into HfO_2 SL, segregation energy is calculated as

$$E_s = E_{m-\text{bulk}} - E_{m-\text{interface}} \tag{5}$$

$E_{m-\text{bulk}}$—energy, when the metalic element is staying the $Hf0_2$.

$E_{m-\text{interface}}$—energy, when the metalic element is staying at the interface.

2.4 Conduction mechanism of resistive switching in binary oxides

The physics involved in an RRAM is a complex procedure. In a binary metal oxide, the switching mechanism is dominated by the ionic effect related to electrochemical reactions to create a CF between two metal electrodes [40, 41]. It is popularly represented as redox/oxidation principles. The CF is formed in a metal oxide RRAM, which leads the memory cell into an LRS. It is observed by using conductive atomic force microscopy (CAFM) in the metal oxides. After the forming operation [42], D.H.Kwon et al. demonstrated the 10-nm diameter CF in a TiOx by high-transmission electron microscopy (HRTEM) [43].

The CF structure development along the switching layer is an unpredictable process. It may vary from the single filament to multiple filament structures, based on that HRS/LRS ratio can change. Mostly in an HfO_2 RRAM cell, monoclinic and amorphous structure [44] stated that Vo creates a defects state in metal oxides. P. Calka confirmed the CF diameter (~ 20 nm) by HRTEM analysis [45]. S. Privitera et al. demonstrated the CF formation by a metallic Hf in an HfO_x RRAM [46]. For an easy method to identify a CF nature, whether the CF behaviors are metal or semiconductor, the temperature versus LRS values is obtained. When the temperature raises, LRS rising, it ensures the metallic nature otherwise semiconducting nature. Many studies show LRS current–voltage (IV) characteristics follow the linear or Ohmic rules.

The HRS IV characteristic of a metal oxide RRAM is a very complex procedure, in which various types of physical phenomena are observed. W.Y. Chang et al. and Y.M. Kim et al. observed Poole–Frenkel emission [47, 48]. Z. Wei et al. and C.Y. Lin et al. noted the Schottky emission [49, 50]. Furthermore, Q. Liu et al. and H.Y. Lee et al. ensured the IV in HRS is based on SCLC [51, 52]. Figure 6 and Table 1 explain all the possibilities of electron transport physical mechanism from cathode to anode [53].

Finally, depending on the dielectric characteristics, bandgap energy, fabrication technology, and the presence of an interface layer, the conducting path and conducting mechanism are varied. Also at a low bias voltage, the IV graph

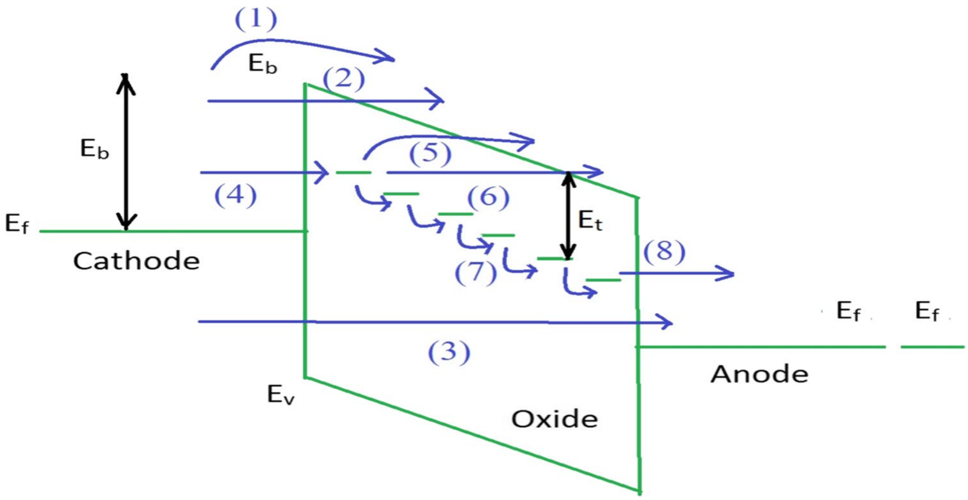

Fig. 6 Possible electron conduction physics in an M-I-M structure [53]

Table 1 Different conduction physics phenomenon in metal oxide RRAM

Number on Fig. 6	Name of the conduction phenomenon	Explanation
1	Schottky emission	Electrons are activated by a thermal process. These activated electrons are introduced above the barrier into the conduction band (CB)
2	Fowler–Nordheim tunneling (FNT)	At the high electric field, an electron can tunnel from the cathode into the CB
3	Direct tunneling	When the metal oxide layer thickness is very thin (< 3 nm), electrons can directly tunnel from the cathode to anode
4	Trap-assisted tunneling (TAT) (Assumption: The oxide layer has enough number of traps)	Step: 1 Tunneling from the cathode to traps
5		Step: 2 Poole–Frenkel emission (Trap to CB)
6		Step: 3 Trap to CB like FNT
7		Step: 4 Mott hopping (Trap to trap hopping or tunneling)

simply follows the fixed electron conduction method of the CF. In the case of high bias voltage, the CF creation/rupture and resistance values are random in nature.

Practically, the current conduction mechanism in RRAM is not a unique description; it varies based on the material structure and other factors. Mi Ra Park et al. fabricated three different devices Pt/Ti/TaO_x/Pt, Pt/Ti/HfO_2/Pt, and Pt/Ti/TaO_y/HfO_2/Pt (D1, D2, and D3 respectively), and in all three devices in LRS, Ohmic conduction is dominant, but in HRS, D1-Poole–Frenkel (PF) and SCLC, D2-Schottky, and D3-Schottky and SCLC [54]. In Wei Zhang et al., trilayer structure [55] shows Ohmic and SCLC in LRS and HRS respectively. Later M.M.Mallol et al. investigated the electrical conduction in a Ni/Al_2O_3/HfO_2/n + -Si stack layer memory cell. They accomplished that in a fresh memory cell, Poole–Frenkel (at the low electric field) and Fowler–Nordheim (at the high electric field) are the dominated conduction mechanisms [56]. Upgrading of Vo yields a conduction change from one switching state to another state. Fang-Yuan conducted experiments in a nitridation-treated Pt/HfO_2/TiN RRAM device. Suggested, after nitridation, at HRS the conduction is switched to Schottky emission from Poole–Frenkel. In LRS, current conduction becomes SCLC from Ohmic, confirmed that defect passivation is the major reason for this conduction switching operation [57].

Andrey et al. experimented and analyzed the current conduction mechanism by changing the switching layer oxidation level (fully, partially, and less) in Ti/HfO_x/Pt structure. They concluded in a fully oxidized (HfO_2) at both LRS and HRS state, Ohmic conduction is responsible. In a partially oxidized state ($HfO_{2\text{-}x}$), trap-filled space charge limited conduction (TF-SCLC) plays a vital role in HRS. Also in a less oxidized state, both HRS and LRS are controlled by the TF-SCLC mechanism [58]. Recently, Muhammad Ismail et al. experimented in TaN/HfO_2/ZrO_2/Pt memory cell. They observed Schottky conduction in its switching state [59].

3 Materials and device structure fabrication

In RRAM literature, a still extensive collection of metal electrodes, insulator switching layers, diverse structure mixture of fabrication techniques are discussed for better device performance. The following sections analyzing the imperative materials which are used in binary metal oxide RRAM applications.

3.1 Switching materials

Among various TMO, HfO_2 is the effective candidate for the RRAM applications due to its valuable properties [60]. Using HfO_2 alone or along with other metal oxide layers (bilayer, trilayer), structures are modified to improve the device efficiency. Recently, the Pt/Ti/HfO_2/TiO_2/TiN, TiN/Ti/HfO_2/Al_2O_3/TiN, and Pt/TiO_2/HfO_2/TiO_2 trilayer structure materials are provided with better device performance [61–63].

3.2 Electrode selection

Various electrode materials are used in HfO_2-based switching materials. Table 2 focuses on the important electrodes involved in the recent literature. From that, mostly and Pt are the imperative metal electrodes. In some devices, only the electron injection process is occurring. The reason is, such devices have an oxygen reactive electrode with less work function value. In the case of non-reactive electrodes with increased work function value devices, both electron injection and (or) electron de-trapping processes occur shown in Fig. 7. This latter principle creates oxygen interstitials and oxygen molecules, which affects the device's uniformity.

B. Traoreet al. experimented and concluded that the TiN/Ti sample has less forming voltage (Vf) in comparison with Pt/Pt. Also, the TiN/Ti sample has a greater current value at the initial stage [64]. Y. Hou et al. fabricated the TiN/HfO_2/Pt resistive switching (RS) devices with TiN top electrodes in a range of Ar: N2 ambient conditions. The electrical parameters are more effective on the ambient Ar: N2 ratio. They concluded by the above process that the crystal orientation can be changed to (200) orientation. In this orientation, the oxygen reservoir capability is high. It leads to high switching stability compared to (111) crystal orientation [65].

Boubacar Traore demonstrated three different electrode combinations of Pt/Pt, Pt/Ti, and TiN/Ti along with the HfO_2 switching layer. They observed oxide reactive electrodes have better thermal and switching stability due to the fewer amounts of oxygen interstitials about a CF region. In non-reactive electrodes, a huge amount of oxygen interstitials presents near the CF that leads to reduced device variability due to the rapid reset process [66].

Also, the effect of the Ti top electrode is verified and shown in Fig. 8. Basic switching parameters are analyzed; it confirmed Ti top electrodes are an improved performance like low forming, set and reset voltage compared with platinum as a top electrode. That can be justified, though the three electrodes have the same physical dimension and fabrication process, in Ti electrode sub-stoichiometric area formed at the Ti/HfO_2 boundary caused by the action of the over Ti metal with oxygen during the device manufacture [67, 68]. Moreover, Po-Hsun Chen et al. used indium-tin-oxide (ITO) as the top metal electrode in HfO_2 RRAM cells. It was reported that ITO provides a valuable performance of high speed (50 ns) and endurance (10^7 cycles). The reason is, compared to a metal electrode (Pt), the ITO electrode permits self-limiting current flow; meanwhile, the forming and set operation, remarkably, no need to use CC limit and it is appropriate for low power consumption applications [69]. J. Muñoz-Gorriz et al. observed the large memory window when Ni is used as a top electrode compared to the Cu electrode [61].C. Vallée et al. [70] investigated the effect of a bottom electrode when using TiN and Pt. Their team concluded that better results were obtained for Pt as a bottom electrode instead of TiN.

Recently, Zhihua Yong et al. analyzed the TiN bottom electrode fabrication processes. ALD fabrication technique TiN-fabricated HfO_2 device yields a reduced forming and switching voltage compared to PVD fabrication techniques [71]. Shih-Kai Lin proved high thermal conductivity electrode Ti gives more oxygen ions. This effect contributes to a complete reset process; it modulated the switching layer thickness gives a fine RS operation [72]. Jianxun Sun, Juan Boon Tan, and Tupei Chen et al. shown three different top electrode combinations are analyzed. The author confirmed that high thermal stability TiN/Ti/TiN electrode structure provides uniform switching by the combined action of TiN (oxygen diffusion barrier during post-metal annealing (PMA), Ti (oxygen exchange layer), and TiN (capping layer to prevent the oxidation of middle Ti layer)[73]. Qiang Wang et al. demonstrated the HfO_2-based RRAM with improved reliability and power consumption. They experimented with the device with the O_3 pre-treatment process on the BE TiN. It leads to the two interfacial layers of TiON and TiO_2 [74]. Zhihua Yong et al. compared the device performance of atomic layer deposition (ALD) processed TiN BE memory cell with sputtered TiN BE. It brings about high switching uniformity with low operating voltages is invented in ALD TiN cells [75].

Table 2 Summary of HfO_2-based switching RRAM device physical and electrical parameters

Structure	Thickness (nm)	CC	Vf (V)	Vset (V)	Vreset (V)	HRS/LRS	Endurace (cycle)	Retention (s)	Reference
$Pt/HfO_2/TiO_2/HfO_2/Pt$	100/5/10/5/30	10 mA	7	1.5	0.7	10^3	$> 10^3$	10^8	[55]
$Pt/Al_2O_3/HfO_2/Al_2O_3/TiN$	100/3/10/6/30	10 mA	− 2	− 1.2	1.38	100	$> 10^3$	10^8	[130]
$TiN/HfO_2/Al_2O_3/TiO_x/IrO_x$	-	–	− 9	− 3.5	3.8	100	10^6	10^4	[146]
$Pt/HfO_2/TiN$	110/23/—	5 mA	7	1	− 1.5	10	10^9	10^4	[57]
$Pt/BN{:}SiO_2/HfO/BN{:}SiO_2/TiN$	200/5/10/5/–	100 µA	2	1	− 1.5	100	10^{12}	-	[145]
$TiN/HfO_2/Ti/TiN$	–/10/5/–-	10 mA	3	0.6	− 1.4	100	10^6	10^8	[147]
$Pt/HfO_2{:}Al{:}TiN$	–-/5.5/–	100 µA	2	0.5	− 0.4	10	10^8	10^6	[148]
$TiN/TaO_x/HfO_2/TiN$	–-/60/8/–-	—-	2.5	1.75	− 1.7	10	10^6	10^4	[135]
$TiN/Ti/HfO_2/Al_2O_3/TiN$	—/–/5/1/–	230 µA	4	2	− 1.3	20	10^6	10^3	[153]
$Pt/Ti/HfO_2/Pt$	35/49/41/34	5 mA	–-	1.1	− 1.2	100	10^2	10^4	[54]
$Pt/TiO_2/HfO_2/TiO_2/Pt$	100/10/10/10/100	15 mA	3.2	1.51	− 0.51	10^3	10^2	10^4	[63]
$TaN/HfO_2/ZrO_2/Pt$	70/6/6/—	10 mA	8	1.2	− 1.3	> 10	10^3	10^5	[59]
$Ti/HfO_2/Ti/TiN$	200/10/50/150	—	− 3	0.5	− 0.8	100	10^4	—	[72]
$Ag/HfO_2/TiN$	50/15/80	10 mA	2	1.5	− 1.5	–	–-	—	[62]
$TiN/Ti/HfO_2/Pt$	60/8/6/50	3 mA	2.5	0.7	− 1.5	50	10^2	10^2	[73]
$TiN/Ti/TiN/HfO_2/Pt$	60/8/4/6/50	3 mA	1.15	0.5	− 1.5	500	10^6	10^3	
$ITO/HfO_x/TiN$	200/7/50	100 µA	0.85	0.11	− 0.15	90	10^6	10^4	[154]
$Pt/TiO_x/HfO_2/Pt$	70/30/3/100	10 µA	3	1.5	− 1.12	~ 10	——-	10^4	[86]
$TiN/HfO_2/TaOx/TiN$	20/10/20/20	100 µA	4	2.7	− 2.5	—-	10^5	10^5	[136]
$TiN/Si/HfO_2/Pt$	40/8/10/70	1 µA	3.5	2.8	− 2.8	~ 10	10^5	10^4	[149]
$Pt/HfO_2/TiON/TiN$	100/9/9/90	1 mA	− 1.8	− 1	0.64	200	10^4	10^4	[74]
$Ti/HfO_2{:}Al/Pt$	50/20/120	2 mA	—	0.5	− 0.9	100	$5*10^2$	10^5	[111]
$ITO/HfO_2/TiN$	20/3.3/30	—	3.8	0.2	− 1.5	100	10^6	10^6	[75]
Pt/YDH/Si	—-	1 mA	− 3.4	− 1.8	0.8	100	$2*10^2$	10^6	[155]
$Al/Ti/HfO_2/Pt$	70/100/18/200	5 mA	8	1.5	− 1.5	50	—	—-	[98]
$Cu/HfO_2{:}Au/Pt$	10/20/–-	100 mA	–-	0.3	− 0.9	100	—	——	[106]
$Ti/AZTO/HfO_2/Pt$	20/35/15/–-	10 µA	–-	1	− 0.5	100	10^7	10^4	[134]
$TiN/HfO_2/Pt$	–/30/–-	1 mA	—-	1	− 2	10	10^5	—-	[65]
$Cu/HfO_x/HfO_x{:}Au/Ti/Pt$	–/10/20/–/–	10 mA	1.2	0.1	− 0.1	10^4	——	10^4	[108]
$TiN/Ti/HfO_x/TiN$	100/10/15/150	1.5 mA	2.04	0.95	− 1.22	100	10^6	10^6	[137]
$Tin/Ti/Tin/HfO_2/W$	40/15/2/5/500	1 mA	3	0.5	− 0.5	25	10^4	—-	[138]
$Cu/Ti/HfO_x/Ti/TiN$	–/–/50/10/100	100 µA	–-	0.8	− 0.4	10^3	–-	—-	[156]
$Pt/Ti/HfO_2/Ti/Pt$	70/5/10/30/70	10 mA	3.2	1.3	− 0.9 to 1.2	100	10^3	10^5	[157]
$Pt/HfO_2/SiO_2/TaN$	100/5/2/–-	10 mA	− 5	− 2.5	3	10^4	10^3	10^4	[152]
$Ta/Ti/HfO_x/Ti/HfO_x/TiN$	80/2/3/2/6/100	1 mA	2.2	1.5	− 2	-	-	-	[94]
$ITO/HfO_2/TiN$	250/8/42	50 µA	–	0.5	− 0.22	20	10^5	10^3	[87]
$Pt/HfO_2/Al_2O_3/TiN$	–/7/3/–	–	− 6	− 1	1.5	10	10^7	10^4	[150]

3.3 Fabrication

Mostly, HfO_2-based switching layers are fabricated using ALD or a sputtering deposition method. Also, the metal layers are fabricated by any physical vapor deposition. Recently, ALD process is dominated in the fabrication of HfO_2-based RRAM. Wei Zhang et al. fabricated [55] $HfO_2/TiO_2/HfO_2$ trilayer structure by ALD using precursor vapor with an effective accuracy thickness control method, and achieved wide-area uniformity, with brilliant three-dimensional conformity, for a layer deposition in a nanoscale [72]. T. Ting-Ting et al., T. Bertaud et al., and T. Nagata et al. used different types of fabrication techniques such as reactive molecular beam epitaxial, sputtering, introducing reactive metal interlayer, and pulsed laser deposition. Still, the optimized fabrication technology to produce a sharp control of oxygen-deficiency profile with a uniform deposition rate is missing [76–78]. To solve these problems, R.W. Johnson

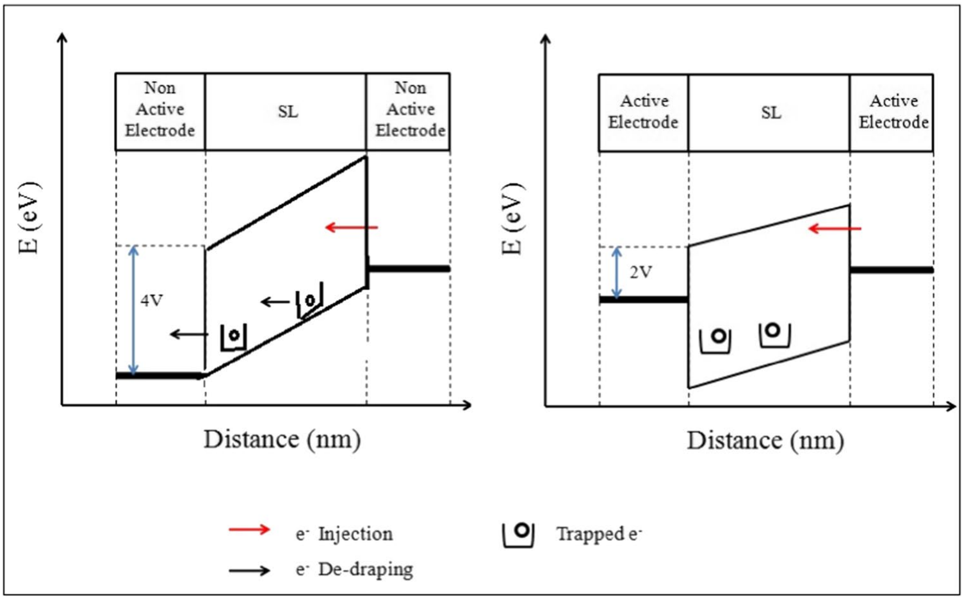

Fig. 7 Electron injection and (or) electron de-trapping processes in a non-active and active electrode

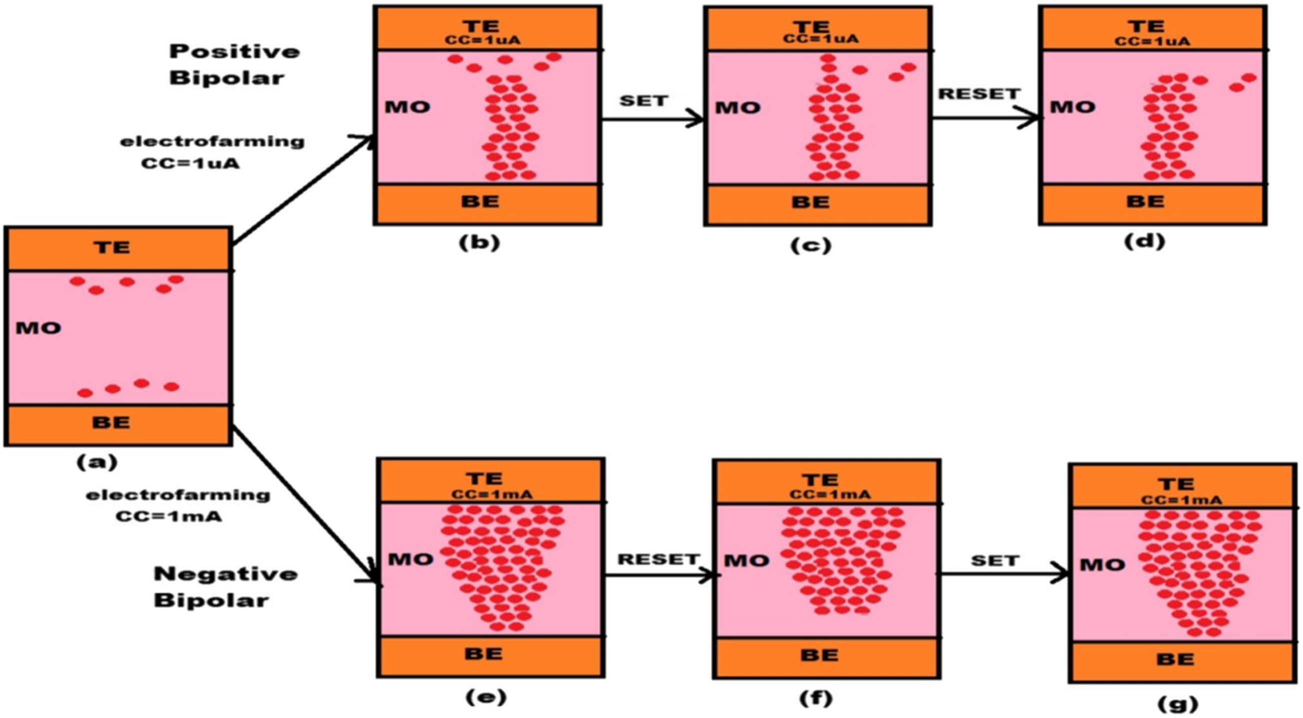

Fig. 8 Schematic diagram of switching operation for different CC values [36]

et al. and H.kim et al. implemented ALD for RRAM fabrication due to its distinctive advantages, specifically self-limiting reaction deposition method, extraordinary conformity on high-aspect-ratio structures, composition, and thickness control at the nanoscale [79, 80].

This research gap accelerated many researchers to work on the ALD process by changing the different conditions like changing the precursor coverage time, varying oxidizer gas type or using an inert gas, controlling the temperature value, and using plasma as a source for metal oxide deposition [81–84]. Recently, Andrey Sergeevich Sokolov et al. investigated the influence of Vo profile on the HfO_{2-x} thin film which is deposited by ALD in the influence of Vo profile, at different precursor times (0.7 to 0.1 s). All, basic RS, I-V characteristics, various electron transport physics, and reliability are analyzed in Ti/HfO_{2-x}/Pt device. Their team suggested, by the modulated ALD vacancy profile, the memory cell power consumption is reduced [85]. Xiangxiang Ding proves controlling the partial pressure of the TiO_2 layer during the sputtering process, and an oxygen vacancy is controlled. High oxygen vacancy leads to quick soft breakdown and high current and high power consumption. Results proved that, with the appropriate partial pressure, it avoids the soft breakdown throughout the entire switching layer that restricts the power consumption [86].

4 Electric characteristics

The device's operating voltages, current, and power are an elemental electric performance metric for a metal oxide RRAM cell. Most of the RRAM need a one-time electroforming operation for set/reset operations until a CF has been formed. The magnitude of the forming voltage leads to a countable effect in a memory cell. Larger forming voltages force the device to more power consumption per cell, reducing this value as much as possible, without affecting other RRAM performance for low power applications.

4.1 Forming voltage vs compliance current

Forming voltage (Vf) affects or is affected by compliance current, metal oxide layer dimensions, HRS, LRS, Vset, Vreset, Ireset, power consumption, random telegraph noise (RTN), temperature, endurance, and retention [36]. Metal oxide RRAM demands a one-time electroforming operation for a successful switching operation. Mostly, the Vf value is higher than the device set and reset voltage values. Vf value is affecting, depending on the device area and electrodes [26, 87–90]. Jingwei Zhanga exposed the RRAM performance for an ITO/HfO_2/TiN structured cell. The ITO is fabricated with an appropriate ratio of In_2O_3:SnO_2 = 9:1. It has more active Sn^{4+} ions that lead to change its valence states comfortably. ITO produces a high stability interface layer in an active electrode metal and oxide interface. This interlayer creation gives rise to excellent reduced switching voltages and reliability in addition to the flexible property [87].

Constantly noted is that, when the device area increasing Vf value decreases, it is a major challenge for device scaling. This scaling threat can be beaten by using local enhancement techniques which is helpful to perform a forming operation in a localized area [91] and by introducing high-permittivity (high k) material as the side-wall spacer structure [15]. The researchers analyzed and confirmed that increased device physical dimension leads to forming voltage reduction. But, as switching layer thickness is increased, Vf also increased [92]. Figure 8 depicts the variation of the CF dimension vs CC. Recently, trilayer annealed Pt/TiO_2/HfO_2/TiO_2/Pt device [63] shows a reduced forming voltage with enhanced reliability for a 15 mA CC value.

4.2 Device dimension vs forming

More researchers have analyzed the device scaling versus forming voltage value. Chen [93] modeled the Vf value for various device dimensions; the expression for forming voltage of area dependence is given by,

$$Vf = C1 - C2\ln(A/a^3) \tag{6}$$

$$C1 = (a/k)\ln(1 - Pf) + (t/k)ln(1/R_0); C2 = a/k \tag{7}$$

where a^3—the volume of one cubic cell which is the smallest part of a device, Pf—probability of forming, A—the area of a device, t—thickness of the device, R_0, k can be assumed from the following resistive transition rate (R) equation that is given by (when applying field is "E")

$$R = R0e^{kE} \tag{8}$$

Figure 9 shows the experimental data that were fitted in the Chen model.

From Fig. 9, when we look for device scaling, Vf is increasing. Though from many experimental data, if we plot the graph Vf versus oxide layer thickness (HfOx thickness), the results are reversed. Reducing the HfOx thickness to less than 3 nm almost forming-free devices can be obtained.

Eduardo P'erez et al. analyzed the forming voltage distribution for three different metal oxide SL (polycrystalline HfO_2, amorphous HfO_2, and aluminum-doped HfO_2) at the wide temperature range of − 40 to 150 °C. A new statistical approach phase-type distribution (PHD) is implemented rather than a conventional Weibull distribution (WD). PHD

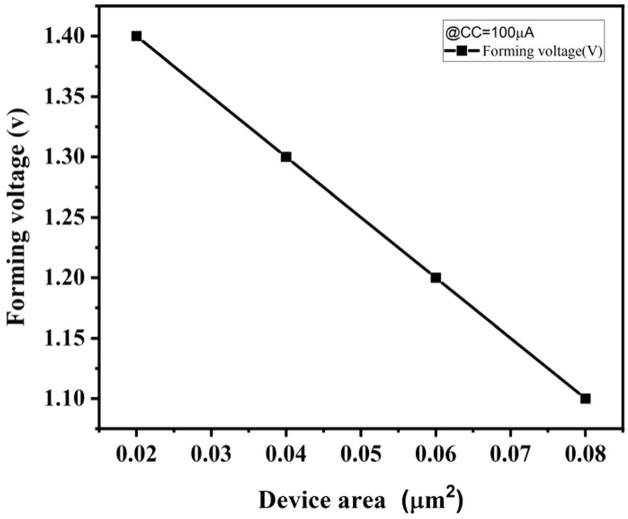

Fig. 9 Chen area scale model (data fitted)

gives more information of intermediate probabilistic states presented in the primary electroforming operation as per the subsequent equation [94]

$$F(V) = 1 - \alpha \exp(TV)e \tag{9}$$

α—($\alpha 1,\ \alpha m$) is a vector components, $T = (qij)i,j = 1\ldots m$ is a matrix of the transient stage i to j, e is a column vector order, and V—voltage.

G. Vinuesa et al. improved the device current conductance linearity into 98.4%. The random nature of conduction is controlled by a cap layer of Ti added in between electrodes and SL. This Ti gives the non-stoichiometric switching action [95].

4.3 Forming-free devices

For commercial memory applications, producing a low power consumption RRAM device is the mandate requirement. As discussed above, the forming operation has taken high-voltage values, which affects the memory cells due to the high electric stress. Anyway, the switching characteristics of the devices typically follow the initial forming process. A. Kalantarian et al. implemented constant voltage stress-forming procedure. Y.-S. Chen et al. established thin HfO_x forming-free devices [96]. Still the deeper perceptive is missing.

4.4 Switching uniformity

The critical mission in RRAM device characteristics is maintaining switching uniformity in intra and inter devices. Researchers are focusing on the improvement of RRAM device switching uniformity, suggested and experimented with various techniques like modifying top electrode [97–99], implanting metal interlayer [100], applying optimized computer-programmed pulses [101, 102], and introducing appropriate dopants [103, 104].

4.4.1 Effect of doping for stable switching

Doping certain metal elements in a metal oxide yields significant effects in the metal oxide RRAM. Since in RRAM, the entire operation is dominated by its CF creation and rupture of CF. With the controlled development of CF, the device switching uniformity can be improved. B. Gao et al. projected that when the trivalent metal is doped in tetravalent metal oxide like HfO_2 and ZrO_2, the formation energy of Vo is reduced. Because of the low formation energy of Vo, CF is formed easily together with dopant atoms which gives high RS uniformity [105]. Tingting Tan et al. fabricated a new device structure Cu/HfO_2:Au/Pt, concluded that the Au doping opposes the random nature of CF formation inside the switching layer, which leads to an improved uniformity, high memory window, and low Vset value. The major reason for this improvement is the formation of an Au-O bond inside the switching layer [106].

Mingyi Rao et al. realized that the Zn-doped HfO_2 RRAM devices show evidence of considerably improved memory performance in terms of its operating voltage and switching uniformity without affecting the endurance. The Zn dopant gives better control over the CF formation which leads the enhanced uniformity [107]. Bai Sun et al. observed high uniformity in an Al-doped HfO_x sample due to the control of Vo by aluminium doping and the high retention value is observed in all samples [108]. Y.C. Yang et al.'s and Q. Liu et al.'s team proved that introducing low valence ions in the film can successfully develop the RS uniformity [109, 110]. Moreover, researchers found that, when nitrogen is doped, all switching and reliability RRAM metrics are improved. Jinfu Lin, Shulong Wang, and Hongxia Liu explored the aluminum-doped HfO_2 SL device structure for multilevel switching operation. Analysis shows that compliance current modulated the switching voltages. This initiates the RRAM device in neuromorphic applications with high uniformity [111].

4.4.2 Stack layer

Using multilayer structure is one of the main techniques which is used to reduce the non-uniformity in the RRAM device [112–118]. The researchers constructed and analyzed the multilayer structure for switching improvement. They reported a multilayer (stack layer) has better switching and reliability characteristics compared to a single layer device [119–126].

H.Y. Lee, L. Chen, and S. Yu et al. suggested the double-layer structure yields better switching uniformity and reduced switching power due to the stable CF creation and rupture [127–129]. Continuously, Cheng C.H and Terai M et al. confirmed the switching improvement in a bilayer device structure [114, 115]. Lai-Guo Wang et al. determined the trilayer-structure oxide-based RRAM devices displayed, suppress the switching value distribution. The cells with a SL structure of Al_2O_3/HfO_2/Al_2O_3 displayed excellent uniformity of set and reset voltages and excellent endurance of switching between the LRS and HRS [130]. Wang LG et al. and H. Lv et al. analyzed the device non-uniformity problem; they concluded that by ion doping or using different material stacks layer, the problem can be solved [131, 132].

Z. Fang et al. reported forming-free RRAM cells with HfOx/TiOx stack layer structure, and both intra-cell and inter-cell uniformity are improved significantly. Compressed set/reset voltage distribution is achieved in that structure. It is justified that, by appropriate Ti doping level and a controlled CF growth mechanism, it leads to the successful uniformity device [133]. Po-Tsun Liu et al. ensured that the multilayer device with Ti/AZTO/HfO_2/Pt structure has high uniformity than a single layer Ti/AZTO/Pt structure. Due to the localized formation of CF ahead of switching uniformity, switching speed (500 ns), endurance (10^7 cycles), and retention (10^4 s) are attributed [134]. Xueyao Huang et al. proposed a unique device structure TiN/TaO_x/HfO_2/TiN to raise the switching uniformity and retention [135]. Xu Zheng et al. tested the fabricated bilayer (HfO_2/TaO_x) RRAM device in a harsh radiation environment. They concluded that after radiation dose, the switching characteristics are not altered. The switching voltage is reduced due to the radiation annealing effect. Moreover, cell uniformity is maintained with a decent value [136].

4.4.3 Other parameters

Maintaining the device uniformity can be done in various ways of ion doping and stack layer. Other technologies were also involved and implemented. Y. Hou et al. demonstrated by an optimized crystal orientation of the top electrode, the oxygen storage capacity is increased; by that high uniform device performance is attributed [65]. Recently, Kai-Chi Chuang et al. analyzed a memory cell structure TiN/Ti/HfO_x/TiN with a fixed enhanced elevated film stack (EFS) novelty structure for a high device-to-device switching uniformity [137] shown in Fig. 10. Moreover, Yichen Fang et al. experimented by inserting a TiN buffer layer, RS stability, and forming voltage is improved [138].

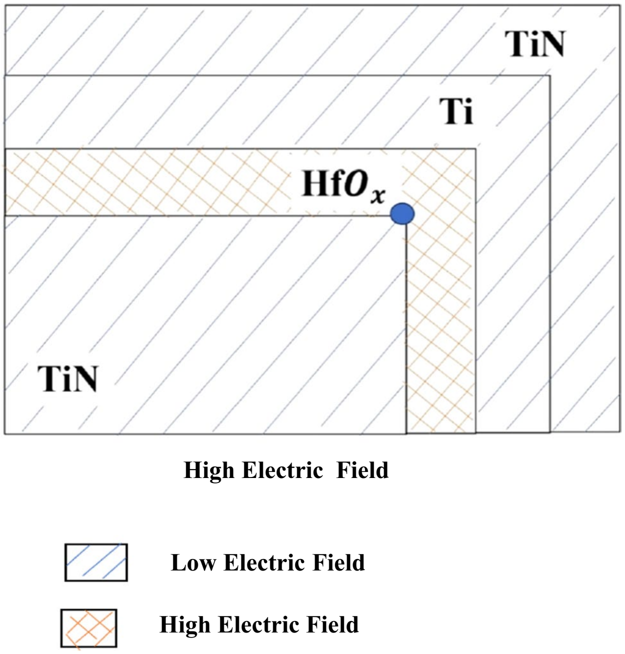

Fig. 10 Electric field distribution in elevated film stack (EFS) structure

Plasma treatment is an attractive technique to enhance uniformity. Bonchoel Ku et al. demonstrated the Ti/HfO_2/Pt/Ti/SiO_2 device, and after the switching layer (HfO_2) fabrication, HfO_2 is subjected to 3 min of Ar plasma treatment. More Vo created in a switching layer, react with Ti produced the TiO_2 interlayer. CF is controlled by that interlayer, and uniformity is improved [139]. Figure 11 explains the CF control action in the Ar plasma–treated and plasma non-treated process.

Producing the local electric field in the SL is an attractive technique to direct the Vo in a controlled manner. Ye Tao et al. constructed a unique structure (Au/HfO_x/MSGC/Pt) with better switching reliability. Mountain-like surface-graphited carbon (MSGC) film is deposited in between SL and BE. The local electric field (LEF) is enhanced as shown in Fig. 12. The creation of random CF formation eliminated also the CF formation and rupture can be controlled easily by that switching uniformity is improved [140].

Also to steady the switching operation and reliability, recently RRAM structure is modified by using sidewall spacer with a high dielectric material instead of a conventional planar structure. Mei Yuvan et al. implemented the sidewall spacer. They introduced a Ta_2O_5 layer as shown in Fig. 13. Results are compared with absences of sidewall structure. Concluded this new structure is confined the electric field for the controlled CF formation and break operation [141].

Recently, Meng Qi et al. also fabricated an Ar surface plasma–treated (SPT) Au/HfO_{2-x}/Pt/Ti/SiO_2 device. They compared the morphological and electrical characteristics of SPT and normal devices. After SPT, the roughness of the switching layer and Vo is increased with a reasonable value. It leads to reduction of forming voltage and avoids the random creation of CF. Furthermore, when the TE is fabricated with tips, LEF directs the CF in a fine-controlled path for high uniformity [142]. Table 2 shows the summary of switching uniformity with an HfO_2 material device structure. Still, the switching uniformity in an HfO_2 RRAM is a bottleneck. Wide research and implementation need by combining various switching uniformity improvement technologies, without affecting other RRAM performance.

5 Reliability

Productive high reliable RRAM performance is the major constraint. Researchers are working to find highly reliable devices by concentrating on the endurance and retention of the device. Both properties are depending on the CF formation and rupture principles. In the literature, to improve the HfO2 material–based reliability, in addition to the experimental procedure, various modeling and simulation

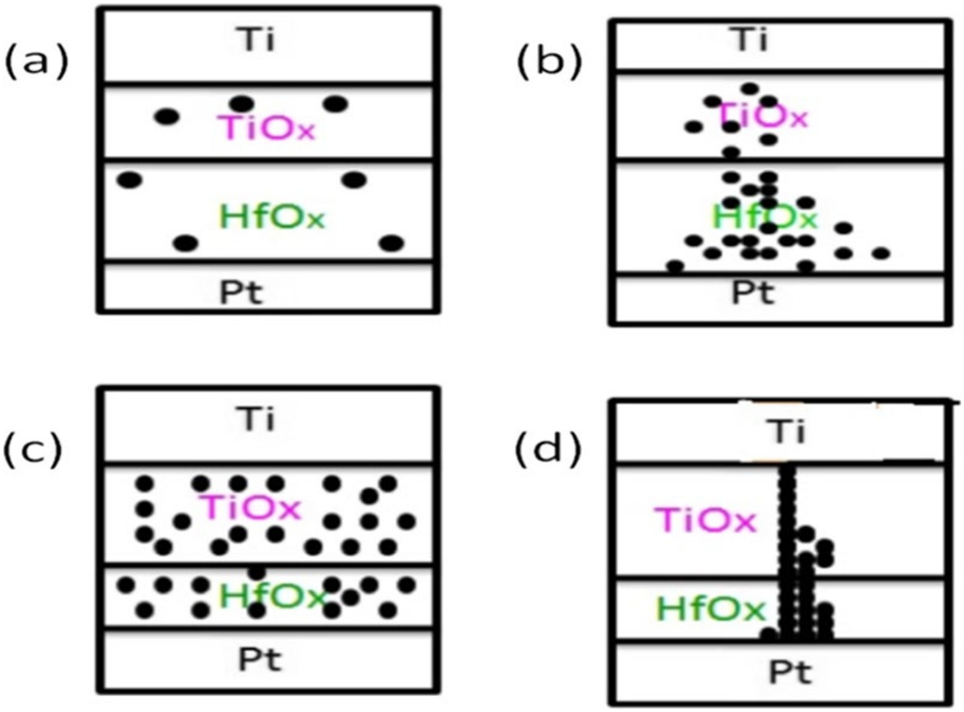

Fig. 11 (**a,b**) Non-Ar plasma and (**c, d**) Ar plasma–treated device

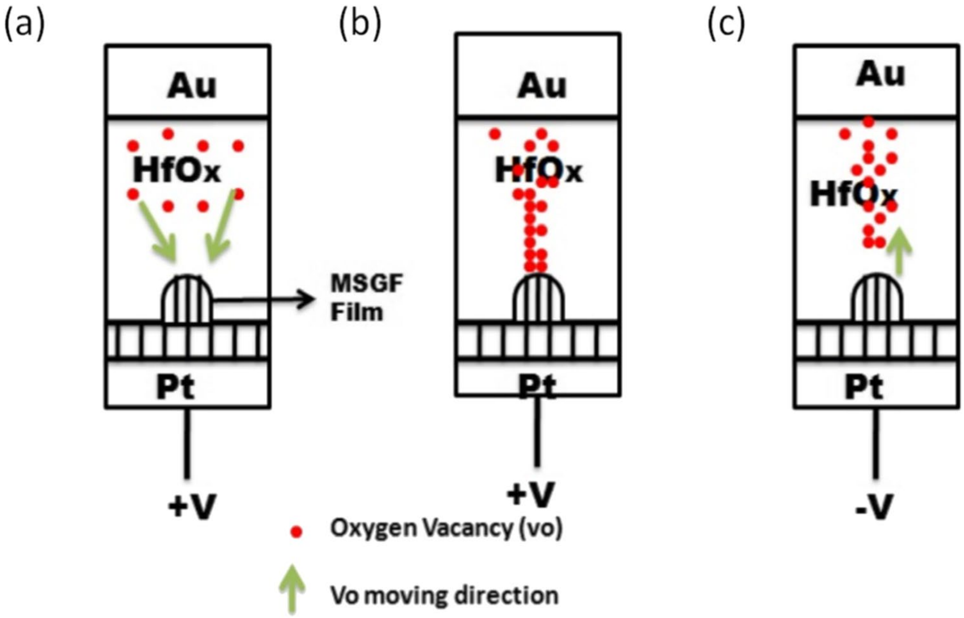

Fig. 12 LEF and controlled CF using MSGC structure. (**a**) Forming. (**b**) Set. (**c**) Reset

techniques are discussed. Debashis Panda et al. reviewed different RRAM models [143].

5.1 Endurance

Jeonghwan Song et al. made the improvement in both retention and endurance characteristics in the HfO_X-based RRAM devices by using the high-pressure hydrogen annealing (HPHA) [144]. According to the HPHA technique, before the top layer deposition, the sample is subjected to high-pressure hydrogen annealing process to amplify the number of Vo inside the switching device. Fang-Yuan Yuan et al. demonstrated the novel idea to increase endurance by applying a nitridation technique. After the switching layer fabrication, the sample is kept inside the solution with urea/ammonia and heated at 160 °C for 30 min. After that, the top electrode is deposited, following the nitridation process, and the endurance increased by 10^9. Also, the retention time is

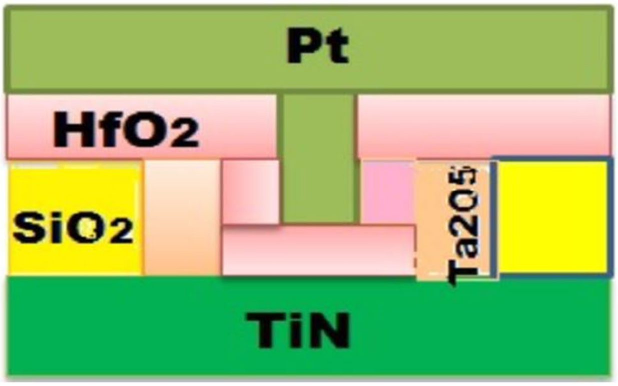

Fig. 13 Schematic diagram of high K space RRAM device

improved by 10^4 s at 85 °C. This improvement is explained by, after the nitridation, the current conduction mechanism in the LRS is changed from Ohmic to space charge limited current (SCLC) principle [57]. A similar type of endurance improvement is observed by Tsung-Ming Tsai et al. in their proposed structure as a new boron nitride (BN) layer is inserted [145]. The Pt/BN:SiO_2/HfO/BN:SiO_2/TiN structure showed high switching endurance 10^{12} cycles with higher stability. This can be explained by the forming process is controlled in a sharp aspect during the redox reaction. In the stack layers, numbers of IL are produced. Creation and rupture of CF in between switching metal oxides and IL layers are quite easy and controllable. So, the memory cells with a stacked structure like Al_2O_3/HfO_2/Al2O3 [130], Pt/HfO_2/TiO_2/HfO_2/Pt [55], TiN/HfO_2/Al_2O_3/TiO_x/IrO_x [146], TiN/TiO_x/HfO_x/TiN [147], and Ti/HfO_2/O_2-HfO_2/TiN [21] demonstrated better uniformity of set and reset voltages and admirable endurance cycles between the LRS and HRS.

In another study, M. Azzaz et al. reported the Vo formation energy is the major endurance improvement. According to their report, high formation energy leads to high endurance and vice versa. It can be observed in HfO_x materials. Higher formation energy leads to thermodynamically encourage HRS. Also, demanded in TiN/Ta_2O_5/Ti/TiN structure, Ta_2O_5 has less formation energy, so the vacancies are more stable in CF. It creates high retention and low endurance [148]. Umesh Chand investigated the influence of the plasma oxidation process on endurance improvement. They optimized their device structure with a Ti/HfO_2 (1 nm)/O_2-HfO_2 (9 nm)/TiN material and dimension. Due to the plasma oxidation (10-min process during the ALD), the oxygen ion concentration is high in a switching layer. Also due to the 1 nm HfO_2 layer, the O_2 ions absorbed by the top electrode were avoided. RS layer provides continuous O_2 ions to the device. The endurance degrade problem is reduced and the endurance value is enhanced by 10^{10} cycle [21]. Xiang ding et al. improved the reliability by adding silicon as an interfacial layer in between the top electrode and SL. Silicon functions as an oxygen scavenger layer. Also, current overshoot is scaled down [149]. Yulin Liu et al. investigated the effects of SL thickness and temperature impact on the endurance performance in a Pt/HfO_2/Al_2O_3/TiN RRAM cell. Results assured when the HfO_2/Al_2O_3 thickness is 7 nm/3 nm, 10^7 cycle endurance attributed with a recognized switching voltage values over a temperature range of 80 °C. More than 80 °C, Vset, Vreset, and Vf are unstable [150].

5.2 Retention

Retention (the capability to store the data for prolonged periods of time in a definite temperature) is an important metric of RRAM measures. Researchers explored and found the track in HRS and LRS retention improvement. To increase the LRS data retention, post-fabrication annealing at 400 °C was proposed to grow the oxygen content in the metal capping layer, also reported creating an interfacial layer between the metal capping layer and the oxide layer that moderates the mobility of the oxygen vacancies. The retention characteristics are reported as a function of baking temperature and aluminum doping concentration for times up to 10^6 s. Disclosed that no considerable changes in LRS, but the noticeable changes are inspected in HRS [151].

Xueyao Huang et al. demonstrated the structure TiN/TaO_x/HfO_2/TiN had brilliant resistance uniformity, endurance, and data retention. Experiments are done with different thicknesses of HfO_2 layers. Finally, concluded that 8 nm HfO_2 thicknesses specify that an optimal thickness exists which gives a good trade-off between forming voltage and data retention [135]. Naga Sruti Avasarala et al. offered a vertical carbon nanotube (VCNT) as a bottom electrode instead of a single layer BE. In their work, they concluded that the switching occurs at the CNT-HfO_2 interface, with a low mobility defect leading to a highly stable defect arrangement that yields the high-temperature retention (> 1300 h @200 °C) [151]. Muhammad Ismail et al. revealed that a high thermal conductivity and lower Gibbs free energy layer of ZrO_2 help for the easy reduction and oxidation and increase the oxygen vacancy generation. It directs the better RS and retention performance [59]. Muhammad Ismail et al. explained the addition of SiO_2(2 nm) layer in between the high oxygen affinity value of TaN electrode and HfO_2 SL, SiO_2 acts as an oxygen reservoir, and it leads to high memory window with a good RRAM switching parameters and high reliability [152]. The trade-off between device structure and reliability is shown in Table 2. From that, simultaneously improving endurance cycle and retention is the challenging work in an RRAM. Still, more researchers are working in the field to give high switching stability with high device variability.

Zhen zhong Zhang, sulphur-doped HfO_x switching layer at 500° C is fabricated. Results show that doping induces more oxygen vacancy in the switching layer. It contributed low power consumption (Pset = 9.08 nJ, Preset = 6.72 nJ) and high switching uniformity, stable endurance, good retention, and high speed (Tset = 6.25 µs, Treset = 7.50 µs) [154]. Yankun Wang et al. researched the united effects of increased oxygen vacancy and the interface formation in yttrium-doped HfO_2 films, accomplish a uniform switching operation [155].

6 Summary and conclusions

Handling huge data and smart devices are in need of high-density nanoscaled non-volatile memory (NVM) with low operating power, monolithic integration, and faster read and write times. Among varied leading upcoming NVM, RRAM is an encouraging technique for forthcoming memory applications due to its high competence, high speed, low power consumption characteristics, and an uncomplicated MIM structure. Predominantly, due to the simple fabrication process, the binary transition metal oxides have largely analyzed for RRAM applications. In specific, HfO_2-based filamentary type RRAM is one of the most descriptive materials due to its outstanding memory performances and CMOS development compatibility. The review starts with the basic principle of RRAM operation, classification of switching mechanism followed by a physical mechanism of resistive switching in HfO_2-based materials. Consequently, the important parameters on RRAM performance including materials selection, device structure fabrication, and forming process have been discussed with their benefits and weaknesses. Finally, this review converges the challenges and possible solutions in HfO_2-based RRAM device for high switching stability and reliability.

Among many electrodes, Pt, TiN, Ni, Cu, and Al are the appropriate metal electrodes for a better RS switching performance and stability with HfO_2 SL. In a fabrication technologies, ALD and sputtering techniques are suitable for highly reliable applications. For low power applications, less forming voltage devices or forming-free devices can be utilized. By optimizing increased device area, reduced SL thickness (Vset and Vreset also reduced), optimized CC value, using polycrystalline structure, increasing the temperature in the forming process, and high rise time of the forming pulse, the Vf value is reduced. The bottleneck of the RRAM device uniformity is improved by using stack layer structures, suitable ion doping, changing the top electrode, inserting metal interlayer, controlling the ALD chamber temperature, and a chemical mechanical planarisation (CMP) process. In reliability concerns, the trade-off between endurance and retention is achieved in various ways. Especially, by nitridation, inserting BN layer, controlling V_{stop} and t_p, applying HPHA fabrication technique, optimal thickness of SL, controlling the CC, concentrating the activation energy of SL, sharp control over the CF size, CF temperature, creating IL in between SL and electrodes and oxygen plasma treatment techniques, post-fabrication annealing process, focusing doping concentration and CNT as an electrode. In the future, for a successful commercial RRAM product, more optimized techniques are needed to improve the switching and reliability parameters. Maintaining the better trade-off between switching stability and device variability directs to implement the RRAM device in an internet of things (IoT) application.

Acknowledgements This work was performed at the VLSI Laboratory for Electronics and Communication Engineering Department, Karunya Institute of Technology and Sciences, Coimbatore, Tamil Nadu, India.

Data Availability Nil.

Declarations

Consent to participate Nil.

Consent for publication Nil.

Conflict of interest The authors declare no competing interests.

References

1. "The International Technology Roadmap for Semiconductors (ITRS),"2013 edition, www.itrs.net. Accessed 6 Jan 2021.
2. R.E. Simpson, M. Krbal, P. Fons, A.V. Kolobov, J. Tominaga, T. Uruga, H. Tanida, Toward the ultimate limit of phase change in Ge(2)Sb(2)Te(5). Nano Lett. **10**(2), 414–419 (2010). https://doi.org/10.1021/nl902777z
3. W. Kang, L. Zhang, J.O. Klein, Y.G. Zhang, D. Ravelosona, W.S. Zhao, Reconfigurable codesign of STT-MRAM under process variations in deeply scaled technology. IEEE Trans. Electron Devices **62**(6), 1769–1777 (2015). https://doi.org/10.1109/TED.2015.2412960
4. X. Fong, Y. Kim, S.H. Choday, S.H. Choday, K. Roy, Failure mitigation techniques for 1T–1MTJ spin-transfer torque MRAM bit-cells. IEEE Trans. Very Large Scale Integ. Syst. **22**(2), 384–395 (2014). https://doi.org/10.1109/TVLSI.2013.2239671
5. H, Ishiwara. "Impurity substitution effects in BiFeO3, thin films—from a viewpoint of FeRAM applications." Curr. Appl. Phys. vol.12, no. 3, pp: 603–611, May. 2012. https://doi.org/10.1016/j.cap.2011.12.019
6. Y. Hayakawa, A. Himeno, R. Yasuhara, W. Boullart, E. Vecchio, W. T. Vandeweyer, T. Witters, D. Crotti, M. Jurczak, S. Fujii, S. S. Ito, Y. Kawashima, Y. Ikeda, A. Kawahara, K. Kawai, Z. Wei, S. Muraoka, K. Shimakawa, T. Mikawa, S. Yoneda, "Highly reliable TaOx, ReRAM with centralized filament for 28-nm embedded application".Vlsi Circuits, *IEEE*. pp: T14-T15, Jun. 2015. https://doi.org/10.1109/VLSIC.2015.7231381

7. W. Wu, H. Wu, B. Gao, N. Deng, S. Yu, H. Qian. "Improving analog switching in HfOx based resistive memory with a thermal enhanced layer." IEEE Electron Device Lett. pp(99):1–1, Jun. 2017. https://doi.org/10.1109/LED.2017.2719161
8. B. Gao, B. Chen, R. Liu, F. Zhang, P. Huang, L. Liu, J. Kang, H. Y. Chen, S. Yu, H. P. Wong, "3-D cross-point array operation on, AlOy/HfOx -based vertical resistive switching memory." IEEE Trans. Electron Devices, vol. 61, no. 5, pp: 1377–1381, May. 2014. https://doi.org/10.1109/TED.2014.2311655
9. U. Russo, D. Ielmini, C. Cagli, A.L. Lacaita, Filament conduction and reset mechanism in NiO-based resistive-switching memory (RRAM) devices. IEEE Trans. Electron Devices **56**(6), 186–192 (2009). https://doi.org/10.1109/TED.2008.2010583
10. A. Fantini, G. Gorine, R. Degraeve, L. Goux, C. Y. Chen, A. Redolfi, S. Clima, A. Cabrini, G. Torelli, and M. Jurczak, "Intrinsic program instability in HfO2 RRAM and consequences on program algorithms." in Electron Devices Meet. pp: 7.5.1–7.5.4, Feb. 2016. https://doi.org/10.1109/IEDM.2015.7409648
11. K.M. Kim, D.S. Jeong, C.S. Hwang, Nanofilamentary resistive switching in binary oxide system; a review on the present status and outlook. Nanotechnology **22**(25), 254002 (2011). https://doi.org/10.1088/0957-4484/22/25/254002
12. H.Y. Jeong, Y.I. Kim, J.Y. Lee, S.Y. Choi, A low-temperature-grown TiO2-based device for the flexible stacked RRAM application. Nanotechnology **21**(11), 115203 (2010). https://doi.org/10.1088/0957-4484/21/11/115203
13. C.H. Huang, J.S. Huang, S.M. Lin, W.Y. Chang, J.H. He, Y.L. Chueh, ZnO1−x nanorod arrays/ZnO thin film bilayer structure: from homo junction diode and high-performance memristor to complementary 1D1R application. ACS Nano **6**(9), 8407–8414 (2012). https://doi.org/10.1021/nn303233r
14. Y.C. Yang, F. Pan, F. Zeng, Bipolar resistance switching in high-performance Cu/ZnO:Mn/Pt nonvolatile memories: active region and influence of Joule heating. New J. Phys. **12**(2), 023008 (2010). https://doi.org/10.1088/1367-2630/12/2/023008
15. Y. T. Tseng, P. H. Chen, T. C. Chang, K. C. Chang, T. M. Tsai, C. C. Shih, H. C. Huang, C. C. Yang, C. Y. Lin, C. H. Wu, H. X. Zheng, S. Zhang, S. M. Sze, "Solving the scaling issue of increasing forming voltage in resistive random access memory using high-*k* spacer structure." Adv. Electron. Mater. vol. 3, p. 1700171, July. 2017. https://doi.org/10.1002/aelm.201700171
16. J. W. Huang, R. Zhang, T. C. Chang, T. M. Tsai, K. C. Chang, T. F. Young, J. H. Chen, Y. C. Pan, X. Huang, F. Zhang, Y. E. Syu, S. M. Sze, "The effect of high/low permittivity in bilayer HfO2/BN resistance random access memory ." Appl. Phys. Lett. vol. 102, no. 20, p. 203507, May. 2013. https://doi.org/10.1063/1.4807577
17. H.F. Tian, Y.G. Zhao, X.L. Jiang, J.P. Shi, H.J. Zhang, J.R. Sun, Resistance switching effect in LaAlO3/Nb-doped SrTiO3 heterostructure. Appl. Phys. A Mater. Sci. Process. **102**, 939–942 (2011)
18. J. Jang, F. Pan, K. Braam, V. Subramanian, Resistance switching characteristics of solid electrolyte chalcogenide Ag2Se nanoparticles for flexible nonvolatilememory applications. Adv. Mater. **24**, 3573–3576 (2012)
19. SeulJi Song, Jun YeongSeok, Jung Ho Yoon, Kyung Min Kim, Gun Hwan Kim, MinHwan Lee, CheolSeong Hwang, Real-time identification of the evolution ofconducting nano-filaments in TiO2 thin film ReRAM, Sci. Rep. 3 (3443) (2013).
20. C.Y. Chen, L. Goux, A. Fantini, S. Clima, R. Degraeve, A. Redolfi, Y.Y. Chen, G.Groeseneken, M. Jurczak, Endurance degradation mechanisms in TiN\Ta2O5\Ta resistive random-access memory cells, Appl. Phys. Lett. 106 (2015), 053501.
21. Umesh Chand, Chun-Yang Huang, Jheng-Hong Jieng,Wen-Yueh Jang, Chen-Hsi Lin,Tseung-Yuen Tseng, Suppression of endurance degradation by utilizing oxygen plasma treatment in HfO2 resistive switching memory, Appl. Phys. Lett. 106(153502) (2015).
22. YuxiangLuo, Diyang Zhao, Yonggang Zhao, Fu-kuo Chiang, Pengcheng Chen,MinghuaGuo, NannanLuo, Xingli Jiang, Peixian Miao, Ying Sun, Aitian Chen, LinZhu, Jianqi Li, WenhuiDuan, JianwangCai, Yayu Wang, Evolution of Ni nano filaments and electromagnetic coupling in the resistive switching of NiO, Nano 7 (642) (2015).
23. M. Kuan, F. Yang, C. Cheng, K. Chen, J. Lee, Key Eng. Mater. 602 (1056) (2014).
24. H-D Kim H-M An 2011 YujeongSeo Tae Geun Kim, Transparent resistive switching memory using ITO/AlN/ITO capacitors, IEEE Electron Device Lett. 32 8 1125 1127
25. H.-Y. Lee et al., IEDM Tech. Dig., p.297, 2008.
26. B. Govoreanuet al., IEDM Tech. Dig., p.729, 2011.
27. Y.-S. Chen et al., IEDM Tech. Dig., p.105, 2009.
28. G. Bersuker et al., "Metal oxide RRAM switching mechanism based on conductive filament microscopic properties," *IEDM Tech. Dig.*, pp.19.6.1–19.6.4, 2010.
29. B. Govoreanu, G. S. Kar, Y.-Y. Chen, V. Paraschiv, S. Kubicek,A. Fantini, I. P. Radu, L. Goux, S. Clima, R. Degraeve, N. Jossart,O. Richard, T. Vandeweyer, K. Seo, P. Hendrickx, G. Pourtois,H. Bender, L. Altimime, D. J. Wouters, J. A. Kittl, and M. Jurczak,"10×10 nm2 Hf/HfO*x*crossbar resistive RAM with excellent performance,reliability and low-energy operation," in *IEDM Tech. Dig.*,Dec. 2011, pp. 31.6.1–31.6.4, https://doi.org/10.1109/IEDM.2011.6131652.
30. S. Yu, Y. Wu, R. Jeyasingh, D. Kuzum, H.-S.P. Wong, An electronic synapse device based on metal oxide resistive switching memory for neuromorphic computation. IEEE Trans. Electron Devices **58**(8), 2729–2737 (2011). https://doi.org/10.1109/TED.2011.2147791
31. D. Kumar, R. Aluguri, U. Chand, T.Y. Tseng, Metal oxide resistive switching memory: materials, properties and switching mechanisms. Ceram. Int. **43**(Supplement 1), S547–S556 (2017)
32. A. Wedig et al., Nanoscale cation motion in TaOx, HfOx and TiOx memristive systems. Nat. Nanotechnol. **11**, 67 (2015)
33. H. Jiang et al., Sub-10 nm Ta channel responsible for superior performance of a HfO2 memristor. Sci. Rep. **6**, 28525 (2016)
34. Wen Sun, Bin Gao, Miaofang Chi , Qiangfei Xia , J. Joshua Yang , He Qian & Huaqiang Wu "Understanding memristive switching via in situ characterization and device modeling" , Nat. Comm. (2019) 10:3453, https://doi.org/10.1038/s41467-019-11411-6.
35. H´ector García , Guillermo Vinuesa , ´Oscar G. Ossorio , Benjamín Sahelices , Helena Cast´an , Salvador Due˜nas , Mireia B. Gonz´alez , Francesca Campabadal, " Study of the set and reset transitions in HfO2-based ReRAM devices using a capacitor discharge" , Solid State Electron. 183 (2021) , https://doi.org/10.1016/j.sse.2021.108113
36. A Napolean, NM Sivamangai, Joel Samuel, Vimukth John, "Overview of current compliance effect on reliability of nano scaled metal oxide resistive random access memory device" 2018 4th Int. Confer. Devices, Circuits Syst. (ICDCS) , 10 January 2019, https://doi.org/10.1109/ICDCSyst.2018.8605178
37. U. Chand, C.Y. Huang, D. Kumar, T.Y. Tseng, Metal induced crystallized poly-Si based conductive bridge resistive switching memory device with one transistor and one resistor architecture, Appl. Phys. Lett. 107 (2015) 203502.
38. Desmond J. J. Loy, Putu A. Dananjaya, Somsubhra Chakrabarti, Kuan Hong Tan, Samuel C. W. Chow,Eng Huat Toh, and Wen Siang Lew, "Oxygen vacancy density dependence with a hopping conduction mechanism in multilevel switching behavior of HfO2-based resistive random access memory devices", ACS Appl. Electron. Mater. 2020, 2, 3160−3170
39. L. Zhua, b, Xuanyu Zhanga, Jian Zhoua, Zhimei Sun, "Interfacial graphene modulated energetic behavior of the point-defect

at the Au/HfO2 interface." Appl. Surf. Sci. **489**, 608–613 (2019). https://doi.org/10.1016/j.apsusc.2019.06.048

40. R. Waser, M. Aono, Nanoionics-based resistive switching memories. Nat. Mater. **6**, 833–840 (2007)
41. R. Waser, R. Dittmann, G. Staikov, K. Szot, Redox-based resistive switching memories - nanoionic mechanisms, prospects, and challenges. Adv. Mater. **21**(25–26), 2632–2663 (2009)
42. J. Y. Son and Y.-H.Shin, "Direct observation of conducting filaments on resistive switching of NiO thin films," Appl. Phys. Lett. vol. 92, no. 22, p. 222106,2008.
43. D.-H. Kwon, K.M. Kim, J.H. Jang, J.M. Jeon, M.H. Lee, G.H. Kim, X.-S. Li, G.-S. Park, B. Lee, S. Han, M. Kim, C.S. Hwang, Atomic structure of conducting nanofilaments in TiO2 resistive switching memory. Nat. Nanotechnol. **5**(2), 148–153 (2010)
44. X. Cartoixa, R. Rurali, and J. Sune, "Transport properties of oxygen vacancy filaments in metal/crystalline or amorphous HfO2/metal structures," Phys. Rev. B, vol. 86, no. 16, p. 165445, 2012.
45. P. Calka, E. Martinez, V. Delaye, D. Lafond, G. Audoit, D. Mariolle, N. Chevalier,H. Grampeix, C. Cagli, V. Jousseaume, and C. Guedj, "Chemical and structural properties of conducting nano filaments in TiN/HfO2-based resistive switching structures.," Nanotechnology, vol. 24, no. 8, p. 085706, 2013.
46. S. Privitera, G. Bersuker, B. Butcher, A. Kalantarian, S. Lombardo, C. Bongiorno, R. Geer, D.C. Gilmer, P.D. Kirsch, Microscopy study of the conductive filament in HfO2 resistive switching memory devices. Microelectron. Eng. **109**, 75–78 (2013)
47. W.-Y. Chang, Y.-C.Lai, T.-B.Wu, S.-F.Wang, F. Chen, and M.-J.Tsai,"Unipolar resistive switching characteristics of ZnO thin films for non-volatile memory applications," Appl. Phys. Lett. vol. 92, no. 2, p. 022110, 2008.
48. Y.-M. Kim and J.-S.Lee, "Reproducible resistance switching characteristics of hafnium oxide-based nonvolatile memory devices," J. Appl. Phys. vol. 104, no. 11, p. 114115, 2008.
49. Z. Wei, Y. Kanzawa, K. Arita, Y. Katoh, K. Kawai, S. Muraoka, S. Mitani, S. Fujii,K. Katayama, M. Iijima, T. Mikawa, T. Ninomiya, R. Miyanaga, Y. Kawashima,K. Tsuji, A. Himeno, T. Okada, R. Azuma, K. Shimakawa, H. Sugaya, T. Takagi,R. Yasuhara, K. Horiba, H. Kumigashira, and M. Oshima, "Highly reliable TaOxReRAM and direct evidence of redox reaction mechanism," IEEE Int. Electron. Devices Meet. pp. 293–296, 2008.
50. C.-Y. Lin, S.-Y. Wang, D.-Y. Lee, T.-Y. Tseng, Electrical properties and fatigue behaviors of ZrO2 resistive switching thin films. J. Electrochem. Soc. **155**(8), H615 (2008)
51. Q. Liu, W. Guan, S. Long, R. Jia, M. Liu, and J. Chen, "Resistive switching memory effect of ZrO2 films with Zr+ implanted," Appl. Phys. Lett. vol. 92,no. 1, p. 012117, 2008.
52. H.Y. Lee, P. Chen, T. Wu, Y.S. Chen, F. Chen, C. Wang, P. Tzeng, C.H. Lin, M. Tsai, C. Lien, HfOx bipolar resistive memory with robust endurance using AlCu as buffer electrode. IEEE Electron Device Lett. **30**(7), 703–705 (2009)
53. Shimeng Yu. "Overview of resistive switching memory (RRAM) switching mechanism and device modeling" 2014 IEEE Int. Symp. Circuits Syst. (ISCAS), 28 July 2014, https://doi.org/10.1109/ISCAS.2014.6865560
54. Mi Ra Park et al. "Resistive switching characteristics in hafnium oxide, tantalum oxide and bilayer devices", Microelectron. Eng. 159 (2016) 190–197.
55. W. Zhang et al., Bipolar resistive switching characteristics of HfO2/TiO2/HfO2 trilayer-structure RRAM devices on Pt and TiN-coated substrates fabricated by atomic layer deposition. Nanoscale Res. Lett. **12**, 393 (2017)
56. M.M. Mallol, M.B. Gonzalez, F. Campabadal, Impact of the HfO2/Al2O3 stacking order on unipolar RRAM devices. Microelectron. Eng. **178**, 168–172 (2017)
57. F.-Y. Yuan et al., Conduction mechanism and improved endurance in HfO2-based RRAM with nitridation treatment. Nanoscale Res. Lett. **12**, 574 (2017)
58. Andrey Sergeevich Sokolov et al. "Influence of oxygen vacancies in ALD HfO2-x thin films on non-volatile resistive switching phenomena with a Ti/HfO2-x/Pt structure", Appl. Surface Sci. 434 (2018) 822–830.
59. M. Ismail et al., Resistive switching characteristics and mechanism of bilayer HfO2/ZrO2 structure deposited by radio-frequency sputtering for nonvolatile memory. Results Phys. **18**, 103275 (2020). https://doi.org/10.1016/j.rinp.2020.103275
60. F. Pan, S. Gao, C. Chen, C. Song, F. Zeng, Recent progress in resistive random access memories: materials, switching mechanisms, and performance. Mater. Sci. Eng. R **83**, 1–59 (2014)
61. J. Muñoz-Gorriz, M.C. Acero, M.B. Gonzalez, F. Campabadal , "Top electrode dependence of the resistive switching behavior in HfO2/n+Si-based devices" , 2017 Spanish Conference on Electron Devices (CDE), April 2017, https://doi.org/10.1109/CDE.2017.7905205.
62. M. Azzaz et al., Improvement of performances HfO2-based RRAM from elementary cell to 16 kb demonstrator by introduction of thin layer of Al2O3. Solid State Electron. **125**, 182–188 (2016)
63. Napolean A, NM Sivamangai, R.Naveenkumar, N.Nithya, "Electroforming atmospheric temperature and annealing effects on 2 Pt/HfO2/TiO2/HfO2/Pt resistive random 3 access memory cell", silicon march 2021
64. B. Traoré, P. Blaise, E. Vianello, E. Jalaguier, G. Molas, J.F. Nodin, L. Perniola, B. De Salvo, Y. Nishi , "Impact of electrode nature on the filament formation and variability in HfO2 RRAM" ,2014 IEEE Int. Reliab. Phys. Symp. July 2014, https://doi.org/10.1109/IRPS.2014.6860676.
65. Y. Hou, R. Liu, W. B. Zhang, L. F. Liu, B. Chen, F. F. Zhang, D. D. Han, J.F. Kang, Y.H. Cheng, "Improved performance of TiN/Hf02/Pt resistive switching device by modifying TiN top electrode crystal orientation" 2014 IEEE Int. Confer. Electron Devices Solid State Circuits, March 2015, https://doi.org/10.1109/EDSSC.2014.7061217.
66. Boubacar Traoré, Philippe Blaise, Elisa Vianello, Luca Perniola, Barbara De Salvo, and Yoshio Nishi, "HfO2-based RRAM: electrode effects, Ti/HfO2 interface, charge injection, and oxygen (O) defects diffusion through experiment and ab initio calculations", IEEE Trans. Electron Devices Vol. 63, No. 1, January 2016.
67. M. Sowinska et al., "Hard X-ray photoelectron spectroscopy study of the electroforming in Ti/HfO2-based resistive switching structures," Appl. Phys. Lett., vol. 100, no. 23, p. 233509, 2012.
68. A. Padovani, L. Larcher, P. Padovani, C. Cagli, and B. De Salvo, "Understanding the role of the Ti metal electrode on the forming of HfO2-based RRAMs," in Proc. 4th IEEE IMW, May 2012, pp. 1–4.
69. Po-Hsun Chen et al." Bulk oxygen–ion storage in indium–tin–oxide electrode for improved performance of HfO2-based resistive random access memory IEEE Electron Device Lett. Vol. 37, No. 3, March 2016.
70. C. Vallée, P. Gonon, C. Jorel, F. El Kamel, M. Mougenot, V. Jousseaume, High j for MIM and RRAM applications: impact of the metallic electrode and oxygen vacancies. Microelectron. Eng. **86**, 1774–1776 (2009)
71. A. Rodriguez, M.B. Gonzalez, E. Miranda, F. Campabadal, J. Suñe, Temperature and polarity dependence of the switching behaviour of Ni/HfO2-based RRAM devices. Microelectron. Eng. **147**, 75–78 (2015)
72. Z. Yong et al., Tuning oxygen vacancies and resistive switching properties in ultra-thin HfO2 RRAM via TiN bottom electrode

and interface engineering. Appl. Surf. Sci. **551**, 149386 (2021). https://doi.org/10.1016/j.apsusc.2021.149386

73. Shih-Kai Lin et al., “Impact of electrode thermal conductivity on high resistance state level in HfO2-based RRAM” , Journal of Physics D: Appl. Phys. https://doi.org/10.1088/1361-6463/ab92c5.
74. Jianxun Sun , Juan Boon Tan, and Tupei Chen, “HfOx-based RRAM device with sandwich-like electrode for thermal budget requirement”, IEEE TRANS. ELECTRON DEVICES, https://doi.org/10.1109/TED.2020.3014846.
75. Q. Wang et al., Interface-engineered reliable HfO2-based RRAM for synaptic simulation. J. Mater. Chem. C **7**, 12682 (2019). https://doi.org/10.1039/c9tc04880d
76. Alessandro Grossi, Eduardo Perez, Cristian Zambelli, Piero Olivo, and Christian Wenger “Performance and reliability comparison of 1T-1R RRAM arrays with amorphous and polycrystalline HfO2” 2016 Joint International EUROSOI Workshop and International Conference on Ultimate Integration on Silicon (EUROSOI-ULIS) , March 2016, https://doi.org/10.1109/ULIS.2016.7440057.
77. T. Ting-Ting, C. Xi, G. Ting-Ting, L. Zheng-Tang, Bipolar resistive switching characteristics of TiN/HfOx/ITO devices for resistive random access memory applications, Chin. Phys. Lett. 30 (2013) 107302.
78. T. Bertaud, M. Sowinska, D. Walczyk, S. Thiess, A. Gloskovskii, C. Walczyk, T.Schroeder, In-operando and non-destructive analysis of the resistive switching in the Ti/HfO2/TiN-based system by hard x-ray photoelectron spectroscopy, Appl. Phys. Lett. 101 (2012), 143501.
79. T. Nagata, M. Haemori, Y. Yamashita, H. Yoshikawa, Y. Iwashita, K. Kobayashi,T. Chikyow, Oxygen migration at Pt/HfO2/Pt interface under bias operation, Appl. Phys. Lett. 97 (2010) 082902
80. R.W. Johnson, A. Hultqvist, S.F. Bent, A brief review of atomic layer deposition: from fundamentals to applications. Mater. Today **17**, 236–246 (2014)
81. H. Kim, W.-J. Maeng, Applications of atomic layer deposition to nano fabrication and emerging nano devices. Thin Solid Films **517**, 2563–2580 (2009)
82. S.-J. Park, J.-P. Lee, J.S. Jang, H. Rhu, H. Yu, B.Y. You, C.S. Kim, K.J. Kim, Y.J. Cho,S. Baik, In situ control of oxygen vacancies in TiO2 by atomic layer deposition for resistive switching devices, Nanotechnology 24 (2013) 295202.
83. R. Zazpe, M. Ungureanu, F. Golmar, P. Stoliar, R. Llopis, F. Casanova, D.F. Pickup, C. Rogero, L.E. Hueso, Resistive switching dependence on atomic layer deposition parameters in HfO2-based memory devices. J. Mater. Chem. C **2**, 3204–3211 (2014)
84. J. Yu, W. Huang, C. Lu, G. Lin, C. Li, S. Chen, J. Wang, J. Xu, C. Liu, H. Lai, Resistive switching properties of polycrystalline HfOxNy films by plasma-enhanced atomic layer deposition, Jpn. J. Appl. Phys. 56 (2017) 050304.
85. J.J. Yang, N.P. Kobayashi, J.P. Strachan, M.-X. Zhang, D.A. Ohlberg, M.D. Pickett, Z. Li, G. Medeiros-Ribeiro, R.S. Williams, Dopant control by atomic layer deposition in oxide films for memristive switches. Chem. Mater. **23**, 123–125 (2010)
86. Andrey Sergeevich Sokolov et al.” Influence of oxygen vacancies in ALD HfO2-x thin films on non-volatile resistive switching phenomena with a Ti/HfO2-x/Pt structure”, Appl. Surface Sci. 434 (2018) 822–830.
87. X. Ding, Y. Feng, P. Huang, L. Liu, J. Kang, Low-power resistive switching characteristic in HfO2/TiOx Bi-layer resistive random-access memory. Nanoscale Res. Lett. **14**, 157 (2019). https://doi.org/10.1186/s11671-019-2956-4
88. Jingwei Zhanga, Fang Wanga,c, Chuang Lia, Xin Shana, Ange Lianga, Kai Hua, Yue Lib, Qi Liub, Yaowu Haoc, Kailiang Zhanga, “Insight into interface behavior and microscopic switching mechanism for flexible HfO2 RRAM” Appl. Surface Sci. 526 (2020), https://doi.org/10.1016/j.apsusc.2020.146723 .
89. S. Koveshnikov, et al., IEDM, 486 (2012).
90. J. Lee, et al., IITC/MAM (2011).
91. H.B. Lv, et al., NVSMW/ICMTD, 52 (2008).
92. W.C. Chien, et al., IEDM, 440 (2010).
93. An Chen “Forming voltage scaling of resistive switching memories” Device Research Conference (DRC), 17 October 2013 pp. 181–182. ECS Trans. 61 (6) 133–138 (2014).
94. A. Chen, Area and thickness scaling of forming voltage of resistive switching memories. IEEE Elec. Dev. Lett. **35**, 57–59 (2014)
95. Eduardo P´erez , David Maldonado, Christian Acal , Juan Eloy Ruiz-Castro , Ana María Aguilera, Francisco Jim´enez-Molinos, Juan Bautista Rold´an, Christian Wenger . “Advanced temperature dependent statistical analysis of forming voltage distributions for three different HfO2-based RRAM technologies” Solid-State Electron. 176 (2021), https://doi.org/10.1016/j.sse.2021.107961
96. G. Vinuesa , O.G. Ossorio , H. García , B. Sahelices , H. Cast´an , S. Due˜nas , M. Kull, A. Tarre, T. Jogiaas, A. Tamm, A. Kasikov, K. Kukli, “ Effective control of filament efficiency by means of spacer HfAlOx layers and growth temperature in HfO2 based ReRAM devices” , Solid-State Electron. 183 (2021), https://doi.org/10.1016/j.sse.2021.108085.
97. Y.-S. Chen, T-Y. Wu, P.-J. Tzeng, P.-S. Chen, H.-Y. Lee, C.-H. Lin, et al., "Forming-free HfO2 bipolar RRAM device with improved endurance and high speed operation," VLSI Techn. Syst. Appl., p. 37, 2009.
98. K.L. Lin, T.H. Hou, J. Shieh, J.H. Lin, C.T. Chou, Y.J. Lee, J. Appl. Phys. 109 (2011)084104.
99. Yanfei Qi, Chun Zhao, Yuxiao Fang, Qifeng Lu, Chenguang Liu, Li Yang and Ce Zhou Zhao “Compliance current effect on switching behavior of hafnium oxide based RRAM”, 2017 IEEE 24th Int. Symp. Phys. Fail. Analys. Integ. Circ. (IPFA), October 2017, https://doi.org/10.1109/IPFA.2017.8060188.
100. L Goux XP Wang YY Chen L Pantisano N Jossart B Govoreanu JA Kittl M Jurczak L Altimine DJ Wouters 2011 Electrochem. Solid-State Lett. 14 H244
101. DS Lee YH Sung IG Lee JG Kim H Sohn DH Ko 2011 Appl. Phys. A 102 997
102. Q. Liu, S.B. Long, W.H. Guan, S. Zhang, M. Liu, J.N. Chen, J. Semicond. 30 (2009)042001.
103. S Balatti S Larenits DC Gilmer D Ielmini 2013 Adv. Mater. 25 1474
104. H.W. Xie, Q. Liu, Y.T. Li, H.B. Lv, M. Wang, X.Y. Liu, H.T. Sun, X.Y. Yang, S.B. Long,S. Liu, M. Liu, “Defects and resistive switching of zinc oxide nanorods with copper addition grown by hydrothermal method” , Semicond. Sci. Technol. 27 (2012) 125008.
105. CS Peng WY Chang YH Lee MH Lin F Chen MJ Tsai 2012 Electrochem. Solid-State Lett. 15 H88
106. B. Gao, H.W. Zhang, S. Yu, B. Sun, L.F. Liu, X.Y. Liu, Y. Wang, R.Q. Han, J.F.Kang, B. Yu, Y.Y. Wang, Symp. VLSI Technol. Honolulu, HI, 2009,p. 30.
107. T. Tan, T. Guo, Xi. Chen, X. Li, Z. Liu, Impacts of Au-doping on the performance of Cu/HfO2/Pt RRAM devices. Appl. Surf. Sci. **317**, 982–985 (2014)
108. Mingyi Rao, Lin Chen *, Qing-Qing Sun, Peng Zhou and David Wei Zhang, A First-principle analysis of resistive switching enhancement of HfO2 thin film induced by zinc doping method, 2014 12th IEEE Int. Confer. Solid State Integ. Circ. Technol. (ICSICT), https://doi.org/10.1109/ICSICT.2014.7021374.
109. Tingting Guo1*, Tingting Tan*, Zhengtang Liu, Bangjie Liu, “Effects of Al dopants and interfacial layer on resistive switching

behaviors of HfOx film", J. Alloys Comp. https://doi.org/10.1016/j.jallcom.2017.02.286.

110. HH. Zhang, B. Gao, B. Sun, G. Chen, L. Zeng, L. Liu, X. Liu, J. Lu, R. Han, J. Kang, and B. Yu, "Ionic doping effect in ZrO2 resistive switching memory," Appl. Phys. Lett., vol. 96, no. 12, p. 123 502, Mar. 2010
111. S. Yu, B. Gao, H. Dai, B. Sun, L. Liu, X. Liu, R. Han, J. Kang, B. Yu, Electrochem. Solid State Lett. **13**, H36–H38 (2010)
112. J. Lin, S. Wang, H. Liu, Multi-level switching of Al-doped HfO2 RRAM with a single voltage amplitude set pulse. Electronics **10**, 731 (2021). https://doi.org/10.3390/electronics1006073
113. J. Yoon, H. Choi, D. Lee, J.-B. Park, J. Lee, D.-J. Seong et al., Excellent switching uniformity of Cu-doped MoOx/GdOx bilayer for nonvolatile memory applications. IEEE Electron Device Lett. **30**, 457–459 (2009)
114. Lin M-H, Wu M-C, Huang C-Y, Lin C-H, Tseng T-Y. High-speed and localized resistive switching characteristics of double-layer SrZrO3 memory devices. J Phys D Appl Phys. 2010;43:295404.
115. C.H. Cheng, A. Chin, F.S. Yeh, Ultralow-power Ni/GeO/STO/TaN resistive switching memory. IEEE Electron Device Lett. **31**, 1020–1022 (2010)
116. M. Terai, Y. Sakotsubo, S. Kotsuji, H. Hada, Resistance controllability of Ta2O5/TiO2 stack ReRAM for low-voltage and multilevel operation. IEEE Electron Device Lett. **31**, 204–206 (2010)
117. F.D. Morrison, D.C. Sinclair, A.R. West, Characterization of lanthanum-doped barium titanate ceramics using impedance spectroscopy. J Am Ceram Soc. **84**, 531–538 (2001)
118. R.-C. Fang, Q.-Q. Sun, P. Zhou, W. Yang, P.-F. Wang, D.W. Zhang, High-performance bilayer flexible resistive random access memory based on low-temperature thermal atomic layer deposition. Nanoscale Res Lett. **8**, 1–7 (2013)
119. I. Kim, J. Koo, J. Lee, H. Jeon, A comparison of Al2O3/HfO2 and Al2O3/ZrO2 bilayers deposited by the atomic layer deposition method for potential gate dielectric applications. Jpn J Appl Phys. **45**, 919–925 (2006)
120. H. Wu, X. Li, F. Huang, A. Chen, Z. Yu, H. Qian, Stable self-compliance resistive switching in AlOδ/Ta2O5 − x/TaOy triple layer devices. Nanotechnology **26**, 35203 (2015)
121. Y. Yang, S. Choi, W. Lu, Oxide heterostructure resistive memory. Nano Lett. **13**, 2908–2915 (2013)
122. X. Chen, W. Hu, S. Wu, D. Bao, Stabilizing resistive switching performances of TiN/MgZnO/ZnO/Pt heterostructure memory devices by programming the proper compliance current, Appl. Phys. Lett. 104 (2014)
123. A.R. Lee, G.H. Baek, T.Y. Kim, W.B. Ko, S.M. Yang, Memory window engineering of Ta2O5 − x oxide-based resistive switches via incorporation of various insulating frames. Sci. Rep. **6**, 1–9 (2016)
124. J.H. Yoon, S. Yoo, S.J. Song, K.J. Yoon, D.E. Kwon, Y.J. Kwon, T.H. Park, H.J. Kim, X.L. Shao, Y. Kim, C.S. Hwang, Uniform self-rectifying resistive switching behavior via preformed conducting paths in a vertical-type Ta2O5/HfO2. ACS Appl. Mater. Interfaces **8**(28), 2–8 (2016)
125. MJ Lee CB Lee D Lee SR Lee M Chang JH Hur Y-B Kim C-J Kim DH Seo S Seo UI Chung I-K Yoo K Kim 2011 Nat. Mater. 10 625 630
126. SH Chang SB Lee DY Jeon SJ Park GT Kim SM Yang SC Chae HK Yoo BS Kang M-J Lee TW Noh 2011 Adv. Mater. 23 4063 4067
127. X. Liu, S.M. Sadaf,M. Son, J. Shin, J. Park, J. Lee, S. Park, H. Hwang, Nanotechnology 22 (2011) 475702.
128. H.Y. Lee, P.S. Chen, T.Y. Wu, Y.S. Chen, C.C. Wang, P.J. Tzeng, C.H. Lin, F. Chen, C.H. Lien, M.J. Tsai, Low power and high speed bipolar switching with a thin reactive Ti buffer layer in robust HfO2 based RRAM, IEDM Tech. Dig. 2008, p. 297.
129. L. Chen, Y. Xu, Q.Q. Sun, H. Liu, J.J. Gu, S.J. Ding, D.W. Zhang, Highly uniform bipolar resistive switching with buffer layer in robust NbAlO-based RRAM. IEEE Electron Device Lett. **31**(4), 356–358 (2010)
130. S. Yu, H.Y. Chen, B. Gao, J. Kang, H.S.P. Wong, HfOx-based vertical resistive switching random access memory suitable for bit-cost-effective three-dimensional cross-point architecture. ACS Nano **7**(3), 2320–2325 (2013)
131. Xu. Lai-Guo Wang, Y.-Q. Qian, Z.-Y. Cao, G.-Y. Fang, A.-D. Li, Wu. Di, Excellent resistive switching properties of atomic layer-deposited Al2O3/HfO2/Al2O3 trilayer structures for non-volatile memory applications. Nanoscale Res. Lett. **10**, 135 (2015)
132. L.G. Wang, X. Qian, Y.Q. Cao, Z.Y. Cao, G.Y. Fang, A.D. Li, D. Wu, Excellent resistive switching properties of atomic layer-deposited Al2O3/HfO2/Al2O3 trilayer structures for non-volatile memory applications. Nanoscale Res Lett **10**, 135 (2015)
133. H. Lv, H. Wan, T. Tang, Improvement of resistive switching uniformity by introducing a thin GST interface layer. IEEE Electron Device Lett. **31**(9), 978–980 (2010)
134. Z. Fang, H. Y. Yu, X. Li, N. Singh, G. Q. Lo, and D. L. Kwong, "HfOx/TiOx/HfOx/TiOx multilayer-based forming-free RRAM devices with excellent uniformity" IEEE Electron Device Letters, vol. 32, no. 4, April 2011.
135. Po-Tsun Liu, Yang-Shun Fan, and Chun-Ching Chen, "Improvement of resistive switching uniformity for Al–Zn–Sn–O-based memory device with inserting HfO2 layer", IEEE Electron Device Lett. vol. 35, no. 12, December 2014.
136. Xueyao Huang, Huaqiang Wu1,, Deepak C Sekar, Steve N Nguyen, Kun Wan1, He Qian, "Optimization of TiN/TaOx/HfO2/TiN RRAM arrays for improved switching and data retention" 2015 IEEE Int. Memory Workshop (IMW), https://doi.org/10.1109/IMW.2015.7150300.
137. Xu Zheng et al., "Back end of line based resistive RAM in 0.13 µm partialy depleted silicon on insulator process for highly relaiable irradiation resistance application" , IEEE Electron Device Lett. https://doi.org/10.1109/LED.2020.3037072.
138. K.-C. Chuang et al., Effects of electric fields on the switching properties improvements of RRAM device with a field-enhanced elevated-film-stack structure. IEEE J. Electron Devices Soc. **06**, 622–626 (2018)
139. Yichen Fang et al. "Improvement of HfOx-based RRAM device variation by inserting ALD TiN buffer layer" IEEE Electron Device Lett. vol. 39, no. 6, June 2018.
140. Boncheol Ku, Yawar Abbas, Andrey Sergeevich Sokolov, Changhwan Choi, "Interface engineering of ALD HfO2-based RRAM with Ar plasma treatment for reliable and uniform switching behaviors" , J. Alloys Comp. 735 (2018) 1181e1188.
141. Ye. Tao et al., Improved switching reliability achieved in HfOx based RRAM with mountain-like surface-graphited carbon layer. Appl. Surf. Sci. **440**, 107–112 (2018)
142. Mei Yuvan et al., "Enhancing the electrical uniformity and reliability of the HfO2-based RRAM using high-permittivity Ta2O5 side wall" , J. Electron Devices Soc. VOLUME 6, 2018.
143. M. Qi et al., Highly uniform switching of HfO2−x based RRAM achieved through Ar plasma treatment for low power and multilevel storage. Appl. Surf. Sci. **458**, 216–221 (2018)
144. Debashis Panda1 , Paritosh Piyush Sahu and Tseung Yuen Tseng " RRAM device models: a comparative analysis with experimental validation", IEEE Access, volume 7, 20 November 2019, 168963 – 168980, https://doi.org/10.1109/ACCESS.2019.2954753
145. Jeonghwan Song et al. "Improvement in reliability characteristics (retention and endurance) of RRAM by using high-pressure hydrogen annealing" , 2014 Silicon Nanoelectronics Workshop (SNW), December 2015, https://doi.org/10.1109/SNW.2014.7348588.

146. Tsung-Ming Tsai et al. , “Controlling the degree of forming soft-breakdown and producing superior endurance performance by inserting BN-based layers in resistive random access memory” , IEEE Electron Device Lett. Vol. 38, No. 4, April 2017.
147. Writam Banerjee, Xumeng Zhang, Qing Luo, Hangbing Lv, Qi Liu, Shibing Long,and Ming Liu, “Design of CMOS compatible, high-speed, highly-stable complementary switching with multi-level operation in 3D vertically stacked novel HfO2/Al2O3/TiOx (HAT) RRAM”, Adv. Electron. Mater. 2018, 1700561, https://doi.org/10.1002/aelm.201700561.
148. Y.S. Chen, H.Y. Lee, P.S. Chen, P.Y. Gu, C.W. Chen, W.P. Lin, W.H. Liu, Y.Y. Hsu, S.S. Sheu, P.C. Chiang, W.S. Chen, F.T. Chen, C.H. Lien, M.-J. Tsai, Highly scalable hafnium oxide memory with improvements of resistive distribution and read disturb immunity, in: Tech. Dig. IEEE Int. Electron Devices Meet. 2009, pp. 95–98.
149. M. Azzaz et al., “Endurance /retention trade off in HfOx and TaOx based RRAM”, 2016 IEEE 8th Int. Memory Workshop (IMW), June 2016, https://doi.org/10.1109/IMW.2016.7495268.
150. Xiang Ding, Xiangyu Wang, Yulin Feng, Wensheng Shen, Lifeng Liu, “Low operation current of Si/HfO2 double layers based RRAM device with insertion of Si film” , Jpn. J. Appl. Phys. https://doi.org/10.35848/1347-4065/ab6b7b.
151. Yulin Liua, Sha Ouyanga, Jie Yang, Minghua Tang, Wei Wang, Gang Li, Zhi Zou, Yifan Liang, Yucheng Li, Yongguang Xiao, Shaoan Yan, Qilai Chen, Zheng Li, “Effect of film thickness and temperature on the resistive switching characteristics of the Pt/HfO2/Al2O3/TiN structure”, Solid State Electron. 173 (2020) https://doi.org/10.1016/j.sse.2020.107880
152. Naga Sruti Avasarala, Marc Heyns, Jan Van Houdt, Dirk J. Wouters , Malgorzata Jurczak “Switching behavior of HfO2-based resistive RAM with vertical CNT bottom electrode” 2017 IEEE Int. Memory Workshop (IMW) **,** 08 June 2017, https://doi.org/10.1109/IMW.2017.7939107
153. M Ismail C Mahata S Kim 2022 Tailoring the electrical homogeneity, large memory window, and multilevel switching properties of HfO2-based memory through interface engineering Appl. Surf. Sci. https://doi.org/10.1016/j.apsusc.2022.152427
154. C. Sun, S.M. Lu, F. Jin, W.Q. Mo, J.L. Song, and K.F. Dong, “The resistive switching characteristics of TiN/HfO2/Ag RRAM devices with bidirectional current compliance” , J Electron. Mater. https://doi.org/10.1007/s11664-019-07069-x.
155. Zhen zhong Zhang et al., “Improvement of resistive switching performance in sulfur-doped HfOx-based RRAM” , Materials 2021,14, 3330. https://doi.org/10.3390/ma14123330.
156. Y Wang et al 2020 Reliable resistive switching of epitaxial single crystalline cubic Y-HfO2 RRAMs with Si as bottom electrodes Nanotechnology https://doi.org/10.1088/1361-6528/ab72b6
157. Feng Yulin, Zhang Kailiang, Wang Fang, Yuan Yujie, Han Yemei, eao Rongrong, Su Shuai, “Improvement on switching uniformity of HfOx-based RRAM device fabricated by CMP” , 2015 China Semicond. Technol. Int. Confer. https://doi.org/10.1109/CSTIC.2015.7153417.
158. Hongwei Xie et al. “Nitrogen-induced improvement of resistive switching uniformity in a HfO2-based RRAM device” , Semicond. Sci. Technol. 27 (2012) 125008 (5pp).